2011 MnROAD Mainline Concrete Construction: Cells 5, 6, and 63

Minnesota Department of Transportation

RESEARCH SERVICES

Office of Policy Analysis, Research & Innovation

Alexandra Akkari, Primary Author
Office of Materials and Road Research
Minnesota Department of Transportation

MnROAD
Office of Materials

December 2012

Research Project
Final Report 2012-37

Your Destination...Our Priority

To request this document in an alternative format, please contact the Affirmative Action Office at 651-366-4723 or 1-800-657-3774 (Greater Minnesota); 711 or 1-800-627-3529 (Minnesota Relay). You may also send an e-mail to ADArequest.dot@state.mn.us.

(Please request at least one week in advance).

Technical Report Documentation Page

1. Report No.	2.	3. Recipients Accession No.
MN/RC 2012-37		

4. Title and Subtitle	5. Report Date
2011 MnROAD Mainline Concrete Construction: Cells 5, 6, and 63	December 2012
	6.
7. Author(s) Alexandra Akkari, Bernard Izevbekhai, and John Siekmeier	8. Performing Organization Report No.
9. Performing Organization Name and Address Minnesota Department of Transportation Office of Materials and Road Research 1400 Gervais Avenue Maplewood, MN 55109	10. Project/Task/Work Unit No. 11. Contract (C) or Grant (G) No.
12. Sponsoring Organization Name and Address Minnesota Department of Transportation Research Services 395 John Ireland Blvd., MS 330 St. Paul, MN 55155	13. Type of Report and Period Covered Final Report 14. Sponsoring Agency Code

15. Supplementary Notes

http://www.lrrb.org/pdf/201237.pdf

16. Abstract (Limit: 250 words)

In September 2011, MnDOT constructed two cells in the MnROAD Mainline in continuation of the study of unbonded overlay (Cell 5) and to facilitate studies on a drainable base (Cell 6) with a longitudinal tined texture. Additionally, roller compacted concrete shoulders were constructed in these cells, to replace the preexisting asphalt shoulders. Finally, repairs were done to a thin concrete overlay of existing asphalt pavement installed in 2004 (Cell 63). This report discusses the construction procedure, instrumentation, and the initial monitoring from these test cells.

17. Document Analysis/Descriptors	18. Availability Statement
Longitudinal tine, Roller compacted concrete, Drainable base, Overlays, Pavement grooving, Subdrains	No restrictions. Document available from: National Technical Information Services, Alexandria, Virginia 22312

19. Security Class (this report)	20. Security Class (this page)	21. No. of Pages	22. Price
Unclassified	Unclassified	96	

2011 MnROAD Mainline Concrete Construction: Cells 5, 6, and 63

Final Report

Prepared by:

Alexandra Akkari
Bernard Izevbekhai
John Siekmeier

Minnesota Department of Transportation
Office of Materials and Road Research

December 2012

Published by:

Minnesota Department of Transportation
Research Services Section
395 John Ireland Boulevard, Mail Stop 330
St. Paul, Minnesota 55155

ACKNOWLEDGEMENTS

Authors gratefully acknowledge contributions to a successful construction project from the following people:

- MnROAD Operations Staff.
- Maureen Jensen and Keith Shannon for their leadership and managerial support.
- Robert Orthmeyer (FHWA) for facilitating the construction of Cell 6.
- Derrick Dasenbrock, Dan Mattison and Dave Borys of the Office of Materials Foundations section for their permeability evaluation of the drainable base.
- Special acknowledgement to Melissa Cole, the project engineer.

TABLE OF CONTENTS

LIST OF FIGURES

LIST OF TABLES

EXECUTIVE SUMMARY

In 2008, unbonded overlays (UBOL) were constructed in cell 5. They consisted of a 4-inch and a 5-inch concrete overlay, 1-inch interlayer of permeable asphalt stabilized stress relief course (PASSRC), and existing concrete pavement. This cell degraded considerably, showing widespread cracking on the leave slab portion of each joint in the 4-inch UBOL. The cracks were much less pronounced, and occasionally nonexistent, in the 5-inch UBOL. To continue the UBOL study, a new initiative replaced the 4-inch concrete overlay and interlayer with 5-inch concrete overlay and a non-woven geofabric. The geofabric was instrumented with moisture and stress sensors to monitor the degree to which 1) the fabric provides stress relief and 2) the fabric provides lateral drainage.

Cell 6 was originally built in 2008 to study thermally insulated concrete pavements (i.e. composite pavements). Due to widespread distress, the cell was reconstructed. Reconstruction included a new drainable base made of a special gradation that balanced porosity and stability. This material was evaluated in lab and field elaborately, and results are discussed in this report. Furthermore, to expand the matrix of surface texture types at MnROAD, a longitudinally tined texture was performed on this cell.

Repair work on Cell 63 was followed by traditional grinding to restore ride. This whitetopping cell was in various stages of surface deterioration prior to the rehab.

Initial monitoring of these test cells included testing for strength, ride quality, on-board sound intensity, friction number, surface texture, nuclear density, and dynamic load testing.

This report is organized in the following manner. Chapter 1 includes the description of the MnROAD test facility, and also describes the techniques used for instrumentation and performance tracking at MnROAD. Chapter two discusses the existing pavements in the test cells that were to be reconstructed, and provides an overview of the design concepts used in the new construction. Chapter three gives specifics on the pavement design and materials, instrumentation, and surface texturing applied to the newly constructed test cells. Chapter four provides a description of both laboratory and field tests procedures, and corresponding results, of the Open Graded Aggregate Base (OGAB) “special.” Chapter five outlines the construction sequence for the base, pavement, shoulders, and demo slabs, and also repairs, required for the test cells discussed in this report. Chapter five also contains initial concrete test results. Chapter six describes the test methods and equipment used for the early performance evaluation of the new construction. This chapter also contains results from the first two rounds of testing up until spring 2012. Finally, chapter seven includes conclusions, recommendations, and lessons learned from these construction projects at MnROAD.

CHAPTER 1: INTRODUCTION

MnROAD Facility

The Minnesota Road Research Project (MnROAD) was constructed by the Minnesota Department of Transportation (MnDOT) in 1990-1993 as a full-scale accelerated pavement testing facility, with traffic opening in 1994. Located 40 miles northwest of St. Paul, MN, MnROAD is one of the most sophisticated pavement test facilities of its type in the world. Its design incorporates thousands of electronic in-ground sensors and an extensive data collection system that provide opportunities to study how traffic loadings and environmental conditions affect pavement materials and performance over time. MnROAD consists of two unique road segments located parallel to Interstate 94. The first is a 3.5-mile Mainline interstate roadway carrying "live" traffic averaging 28,500 vehicles per day with 12.7% trucks. The second is a 2.5-mile closed-loop Low Volume Road which carries a MnROAD-operated 18-wheel, 5-axle, 80,000-lb tractor-semi-trailer to simulate the conditions of rural roads.

Over time, many of the original test sections (cells) have met the end of their service life. Several new research opportunities have been constructed at MnROAD since 2007.

Each MnROAD test cell is approximately 500 feet long. Subgrade, aggregate base, and surface materials, as well as, roadbed structure and drainage methods vary from cell to cell. All data presented herein, as well as historical sampling, testing, and construction information, can be found in the MnROAD database and in various publications. Layout and designs used for the Mainline and Low Volume Road are shown in Appendix A. Additional information on MnROAD can also be found on its web site at http://www.dot.state.mn.us/mnroad/index.html.

MnROAD Instrumentation and Performance Database

Data collection at MnROAD is accomplished with a variety of methods to help describe the pavement response to loads and the environment and the actual pavement performance. Layer data is collected from a number of different types of in situ instrumentation located throughout the pavement surface and sub-layers. The instrumentation measures variables such as temperature, moisture, strain, deflection, and frost depth. Data flows from this instrumentation to several roadside cabinets, which are connected by a fiber optic network that is fed into the MnROAD database for storage and analysis. MnROAD staff also monitors pavement performance on a regular basis, and the data is input into the database. Monitoring data includes ride, distress, rutting, faulting, friction, deflection (FWD), forensic trenches, and material laboratory testing. Data from the sensors or monitoring activities can be requested from the MnROAD database by contacting MnDOT researchers.

CHAPTER 2: PROJECT BACKGROUND

Pavement Condition Prior to 2011

Thin Unbonded Overlay

Cell 5 was reconstructed in 2008 as a thin unbonded concrete overlay over an original 7.5-inch thick concrete pavement test section. The two PCC overlay thicknesses were 5 inches (Cells 305/405) and 4 inches (Cells 105 / 205). The 4" sections had cracked significantly by 2010, with many interconnecting corner cracks in the concrete panels. Although numerous, the cracks did not appear to be rapidly deteriorating. The cause for the early cracking was assumed to be related to the excessive panel size to slab thickness ratio. The panel sizes in the overlay were sawn at 14 feet wide in the driving lane (13 feet wide in passing lane) by 15 feet long. This design was intentional in that researchers wanted to demonstrate that there continues to be definite limits on the panel size to thickness ratio. Engineers today often strive to reduce the amount of joints in concrete pavements to reduce the potential for numerous joint repairs in the future.

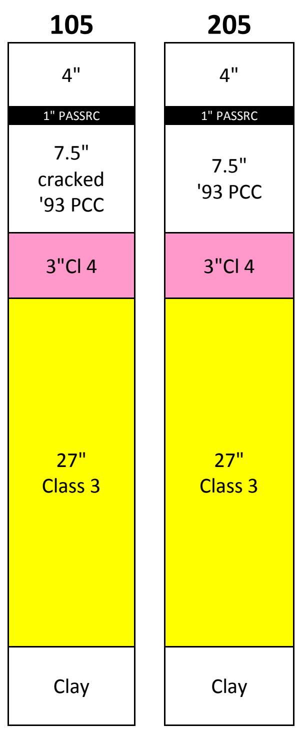

Figure 1: Cell 5 Cross Section Prior to 2011

Composite Pavement (Thin Concrete with Bituminous Surface)

Cell 6 was reconstructed in 2008 as a new composite pavement, made up of a concrete pavement with design thickness of 5-inch overlaid immediately with a 2-inch asphalt surface before opening to traffic. There were stability issues during construction related to a soft clay subgrade, necessitating the addition of a virtually impermeable granular layer directly underneath the concrete. Furthermore, the pavement has shown premature transverse and longitudinal cracks due to heavy traffic loads on a thin pavement. The concrete panel size was 15 feet long by 12 feet wide, which like Cell 5 is probably too large for a 5-inch concrete pavement. Pavement thickness was highly variable during construction, which has led to numerous full-depth repairs. During repairs of the section it was noted that some areas had only a 3.5-inch concrete section which contributed to a general structural failure.

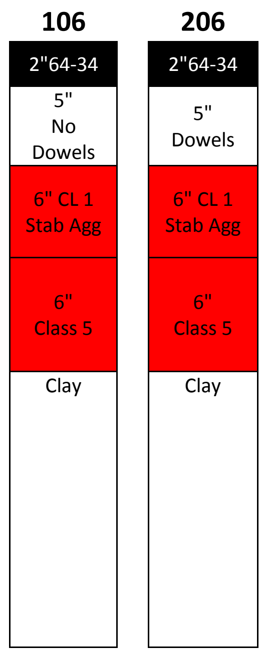

Figure 2: Cell 6 Cross Section Prior to 2011 Construction

Rehabilitation

Cell 63 was constructed in 2004 as an ultrathin concrete overlay of existing asphalt (whitetopping).   The design consisting of 4-inch thick, 5 feet long by 6 feet wide panels, which supplemented research on a previous ultrathin whitetopping test cell consisting of smaller 4 by 4 feet panels. Although the same design as test Cell 62 (sealed joints), Cell 63 was constructed with unsealed joints. It appears the unsealed joints had a major negative impact on the performance of Cell 63. There were numerous cracked and shattered panels in Cell 63, approximately 40 of which needed replacement. This is out of a total of 180 panels. The trend toward a significantly increasing amount of highly distressed panels closely follows the performance curves observed in previous 4-inch thick MnROAD whitetopping test sections.

To ensure continued operation of the mainline test cells at MnROAD, several severely cracked panels had already been replaced with full-depth full size panel repairs.

Steps to slow the rate of deterioration in the panels had been completed in the fall of 2010 to increase the feasibility of the continued operation of Cell 63. These steps included sealing the existing joints to reduce further moisture damage, and injecting materials (high molecular weight methacrylate) to reestablish interlayer bonding of the panels and the underlying asphalt.

Figure 3: Cell 63 Cross Section Prior to 2011

Overview of New Construction

Four test cells at MnROAD were in need of reconstruction or substantial repairs in 2011. Funding from FHWA and MnDOT Innovation Funding provided the opportunity to enhance the research program at MnROAD with several initiatives. These initiatives included the following

a) Use of non-woven geotextiles in thin (5”) unbonded concrete overlay.
b) Smaller panel sizes for unbonded overlays than currently found at MnROAD.
c) Longitudinally tined concrete pavement.
d) OGAB (open graded aggregate base) special.
e) Roller compacted concrete (RCC).
f) Repair of thin concrete overlays.

Input was received from our industry partners, including the Concrete Paving Association of Minnesota (CPAM) and the Aggregate and Ready-Mix Association of Minnesota (ARM), and theywere engaged in the decision making process as we considered MnROAD reconstruction opportunities in 2011.

Non-woven Geotextiles in Thin Unbonded Concrete Overlay Study (Cells 505 and 605)

Due to the cracking in the panels, failure was eminent and presented the opportunity to replace this section with a 5” unbonded concrete overlay using a non-woven geotextile and smaller panel sizes. Use of a non-woven geotextile has become more common and through this research it may prove to be an opportunity to save money by using the geotextile with thinner concrete sections.

Smaller Panel Sizes on Unbonded Overlays Study (Cells 505 and 605)

The previous thin unbonded overlay sections at MnROAD were constructed in 2008 with panel sizes of 14 x 15 in the driving lane and 13 x 15 in the passing lane and a PASSRC interlayer. The panels in the new UBOL were designed to be 6 feet long by 7 feet wide (driving lane) and 6.5 feet wide (passing lane).

Longitudinally Tined Concrete Pavement Study (Cells 306 and 406)

On a few occasions, MnDOT has constructed longitudinally tined concrete pavements, but in recent years has moved to a longitudinal astroturf drag. While the turf drag has proven to be a safe, durable surface in Minnesota, many other states still use longitudinal tining on concrete pavements, which is perceived to show benefits in terms of skid resistance and noise reduction. This cell included a longitudinal tined surface. Specifications were obtained from the CP Tech Center.

OGAB Special Study (Cells 306 and 406)

Over the years MnROAD has shown that both asphalt and concrete pavements perform significantly better when there is some means of draining water that gets into the pavement system. This has been done efficiently by either edge drains or open graded base materials, both of which come at a substantial cost. MnROAD has recently been investigating more cost effective methods of draining water from underneath the pavement surface. This project provides a way to study subsurface drainage and stability under construction to develop a new permeable base material with stability during construction.

Roller Compacted Concrete (RCC) Study (Cells, 306, 406, 505, and 605)

Roller compacted concrete is another relatively new technology that MnDOT incorporated into this project. RCC has many of the desirable properties of typical concrete pavements (i.e., high flexural and compressive strength, low permeability, long term durability) while at the same time its ease of construction (i.e., no steel reinforcing or dowels, no forms or finishing) puts RCC on par with constructing HMA pavements. If the roller compacted concrete performs well on the shoulders at MnROAD, the concrete paving industry will have another tool as an alternative to asphalt shoulders.

Rehabilitation of Cell 63

Information about the techniques and longevity of repairs to thin whitetopping is often requested. Therefore the 2010 condition of Cell 63 provided a unique opportunity to gather such information. A typical concrete pavement rehabilitation (CPR) project will be conducted on the thin whitetopping. After the panel repairs on Cell 63, the surface was diamond ground in the traditional configuration to restore smoothness and skid resistance. The adjacent whitetopping Cell 96, built in 1997, was also diamond ground to eliminate faulting in the concrete panels.

CHAPTER 3: RECONSTRUCTION: DESIGN AND MATERIALS

Cell Overview and Strategy

Cells 105 and 205 were repaired with a 5-inch unbonded overlay utilizing a non-woven geotextile fabric as a stress relief layer. As shown in the Figure 1 below, these cells are now designated as cells 505 and 605 respectively. The existing substrate in cell 505 was noticeably more cracked than that in cell 605. Both 505 and 605 have 6 feet by 7 feet (driving), and 6.5 feet (passing) wide panels. No dowels were used in these cells. Both 505 and 605 were finished with a transverse broom texturing. RCC shoulders were placed on both 505 and 605. Transverse joints were saw cut in the shoulders of Cell 505 to match the Mainline joints, while no joints were sawn in the RCC shoulders on Cell 605.

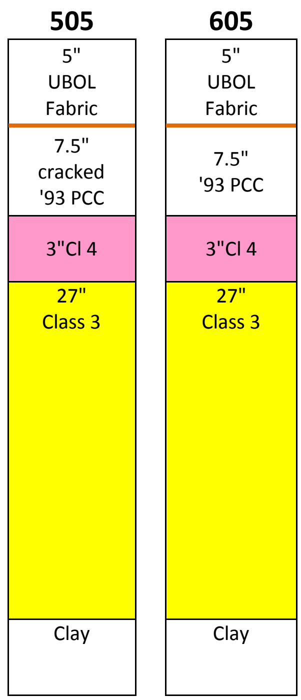

Figure 4: Cell 5 Cross Section

Cells 106 and 206 were removed and replaced with new concrete test sections 306 and 406 respectively. These test sections utilized 6 inches of an OGAB Special base under 6 inches of concrete pavement. Both 306 and 406 were finished with a longitudinal tine surface. The cross section of these test cells is shown in Figure 5. These cells have 15 ft long by 12 ft wide panels with 1-inch dowels, and also have RCC shoulders. The shoulders were sawcut that same as 505 and 605.

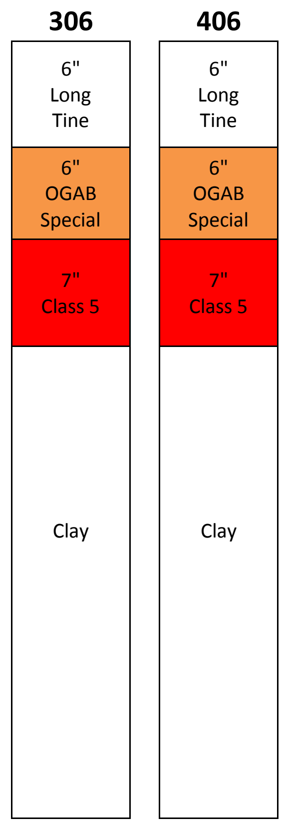

Figure 5: Cell 6 Cross Section

Design

Failure of the 12 foot by 15 foot panels in the 4-inch portion of cell 5 indicated that the 4-inch thickness was probably not stiff enough for the panel size. It was also possible that composite action was lost when the panel cracked considerably downstream of each joint. The new initiative changed the interlayer to a non-woven geofabric and replaced concrete with 5-inch thick panels, with 6 by 7 (driving) and 6.5 (passing) foot spatial dimensions. (The concrete was a minimum of 5 inches thick, but did vary to correct for cross slope. The underlying cross slope was less than the finished slope). The arrangements facilitated the study of effect of fabric interlayer. The major design in cell 6 was the drainable base. It was a modification of the Open Graded Aggregate Base (OGAB) with details shown in Figure 11 in the following chapter.

Concrete Mixes

Cell 5

The concrete overlay in Cell 5 followed the mix designs and material specifications provided in tables 1 and 2.

Table 1: Cell 5 Mix Design

Water	240
Cement	400 (74%)
Fly Ash	140 (26%)
Total Cementitious	540
W/CM	0.44
Sand #1	1218 (40%)
CA #1	914 (30%)
CA #2	914 (30%)
Air Content	7.0%
Slump Range	1" – 3"
Admin #1 Dos Range	0 – 10
Admin #2 Dos Range	0 – 10
Admin #3 Dos Range	0 – 5
Admin #4 Dos Range	0 – 5

Table 2: Cell 5 Material Information

	CA #1	CA #2	Sand #1
Pit Number	73006	71041	71041
Pit Name	Marietta	Elk River	Elk River
Size/Fraction	3/4+	3/4-	Sand
Specific Gravity	2.68	2.69	2.63
Absorption	0.003	0.013	0.009
Aggregate Class	A	C	

Cell 6

The full-depth concrete pavement in cell 6 followed the mix designs and material specifications provided in tables 3 and 4, where the only difference from cell 5 is the aggregate type and proportions. The mix designs and material specifications are provided below.

Table 3: Cell 6 Mix Design

Water	240
Cement	400 (74%)
Fly Ash	140 (26%)
Total Cementitious	540
W/CM	0.44
Sand #1	1223 (40%)
CA #1	612 (20%)
CA #2	1223(40%)
Air Content	7.0%
Slump Range	1” – 3”
Admin #1 Dos Range	0 – 10
Admin #2 Dos Range	0 – 10
Admin #3 Dos Range	0 – 5
Admin #4 Dos Range	0 – 5

Table 4: Cell 6 Material Information

	CA #1	CA #2	Sand #1
Pit Number	71041	71041	71041
Pit Name	Elk River	Elk River	Elk River
Size/Fraction	3/4+	3/4-	Sand
Specific Gravity	2.73	2.69	2.63
Absorption	0.010	0.013	0.009
Aggregate Class	C	C	

Roller Compacted Concrete

American Engineering Testing developed the following mix design for the contractor for the roller compacted concrete (RCC) shoulders in cells 5 and 6.

Table 5: RCC Mix Design

Water	180
Cement	353 (75%)
Fly Ash	117 (25%)
Total Cementitious	470
W/CM	0.38
Sand #1	655(20%)
Sand #2	982 (30%)
CA #1	1637 (50%)
Air Content	7.0%
Slump Range	1/2” – 1”
Admin #1 Dos Range	0 – 10
Admin #2 Dos Range	0 – 10
Admin #3 Dos Range	0 – 5
Admin #4 Dos Range	0 – 5

Table 6: RCC Material Information

	CA #1	Sand #1	Sand #2
Pit Number	71041	19004	71041
Pit Name	Elk River	Lakeville E.	Elk River
Size/Fraction	3/4-	P. Grit	Sand
Specific Gravity	2.69	2.66	2.63
Absorption	0.013	0.009	0.009
Aggregate Class	C		

All Mixes

The following table provides material sources and specification for all cells constructed during reconstruction.

Table 7: Additional Material Notes

	Manufacturer/Supplier	Mill/Pant/Admix Name	Type/Class	Specific Gravity
Cement	Holcim	STGBLMO	I/II	3.15
Fly Ash	Headwaters	COCUNND	C/F	2.50
AEA- Admix #1	Sika Corporation	SIMUAIR25	AEA	
Admix #2	Sika Corporation	SIMUAIR25	AEA	
Admix #3	Sika Corporation	SIKA686	Type A	
Admix #4	Sika Corporation	SIPC161	Type A	

Geotextile Fabric Interlayer Specifications

Table 8: Geotextile Specifications

Property	Requirements	Test Procedure
Geotextile type	Nonwoven, needle-punched geotextile, no thermal treatment (calendaring or IR)	Manufacturer Certificate of Compliance
Color	Uniform/nominally same-color fibers	Visual Inspection
Mass per unit area	≥ 450 g/m^2 (13.3 oz/yd^2) ≤ 550 g/m^2 (16.2 oz/yd^2)	ASTM D 5261
Thickness under load (pressure)	[a] At 2 kPa (0.29 psi): ≥ 3.0 mm (0.12 in) [b] At 20 kPa (2.9 psi): ≥ 2.5 mm (0.10 in) [c] At 200 kPa (29 psi): ≥ 1.0 mm (0.04 in)	ASTM D 5199
Wide-width tensile strength	≥ 10 kN/m (685 lb/ft)	ASTM D 4595
Maximum elongation	≤ 60%	ASTM D 4595
Water permeability in normal direction under load (pressure)	At 20 kPa (2.9 psi): ≥ 1x10-4 m/s (3.3x10-4 ft/s)	Mod. ASTM D 5493 or ASTM D 4491
In-plane water permeability (transmissivity) under load (pressure)	[a] At 20 kPa (2.9 psi): ≥ 5x10-4 m/s (1.6x10-3 ft/s) [b] At 200 kPa (29 psi): ≥ 2x10-4 m/s (6.6x10-4 ft/s)	Mod. ASTM D 6574 or ASTM D 4716
Weather resistance	Retained strength ≥ 60%	ASTM D 4355 @ 500 hrs. exposure
Alkali resistance	≥ 96% polypropylene/polyethylene	Manufacturer certification of polymer

Instrumentation Infrastructure

General Sensor Description and Key

Both cells 5 and 6 were equipped with instrumentation to monitor temperature, moisture, and strain over time. The vibrating wire strain gauge measures strain in the pavement due to material shrinkage and environmental factors. The concrete embedment strain gauge measures the pavement response to dynamic loads. The strain gauges were placed at different depths within the concrete pavement layers. The humidity and temperature (thermocouple) sensors were placed at different depths throughout the pavement, base, and subgrade using MnROAD designed sensor trees. The general instrumentation layout is shown in the figures below.

Table 9: Instrumentation Layout Key

Symbol	Description
	Moisture Tree
	Longitudinal VW
	Transverse VW
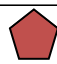	Thermocouple Tree
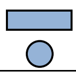	Pore Water Pressure Sensor
	Conduit Run
	Dynamic Strain Gauge
	Underlying Pvmt. Edge/Joint
	Lead Wires
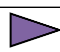	Moisture Sensor
	Thermocouple

Cell 6 Sensor Layout

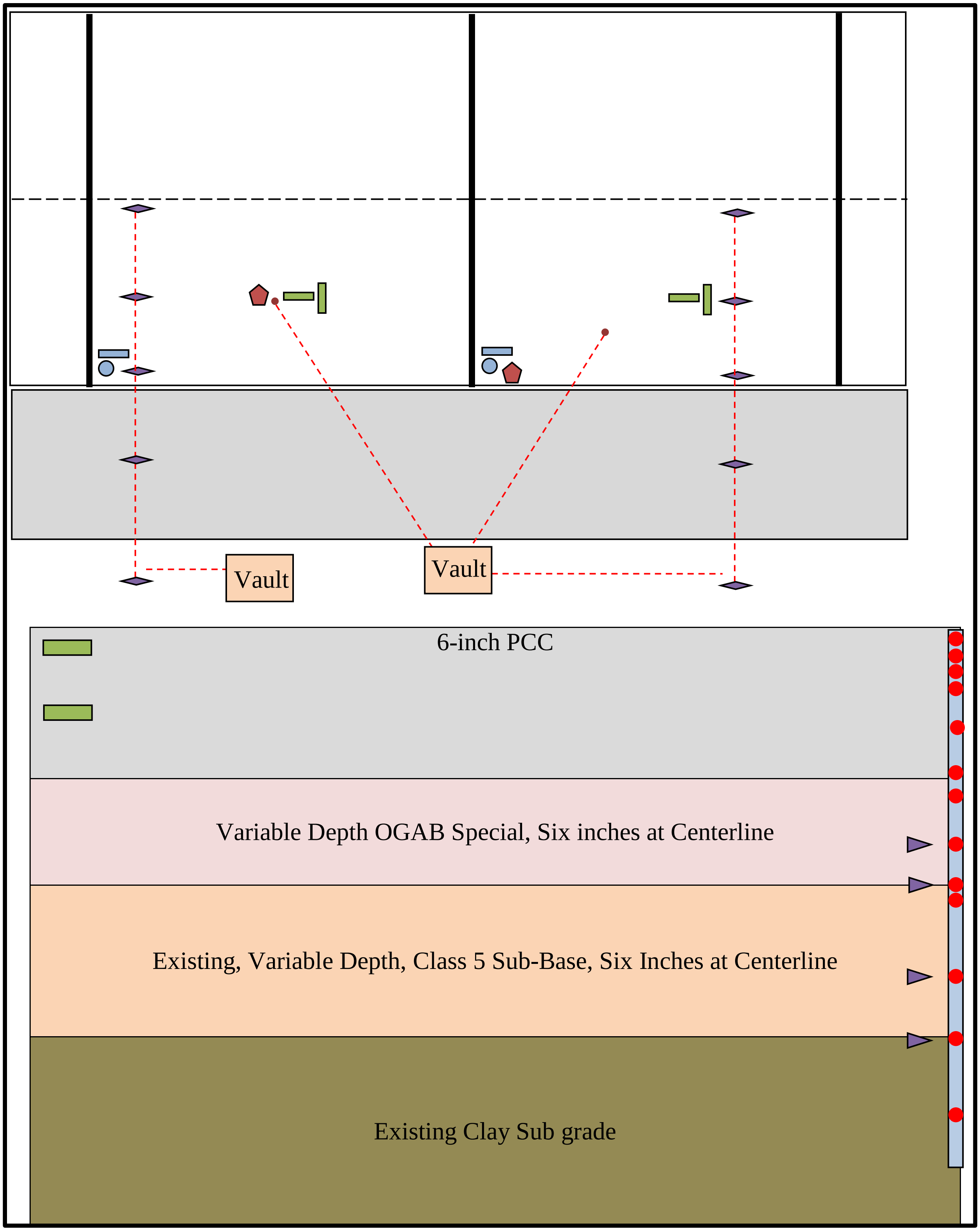

Figure 6: Cell 6 Instrumentation Layout

Table 10: Cell 6 Sensor Description

Code	Quantity	Sensor	Description
MH	8	Relative Humidity	Sensirion, SHT75, Humidity/Temperature Sensor Assembly
TH	8	Temperature	Sensirion, SHT75, Thermistor
PW	4	Pore Pressure	Geokon 3410, Pore Water Pressure Sensor
WM	32	Resistance/MC	Irrotometer, Watermark 200SS, Soil Water Tension/Resistance
TC	20	Temperature	Omega Thermocouple Extension Cable, 1@12 Pair and 1@8 Pair
VW	8	Static Strain	Geokon, Vibrating Wire Strain Gauge
XV	8	Temperature	Geokon, Vibrating Wire Strain Gauge Thermistor

Cell 5 Sensor Layout

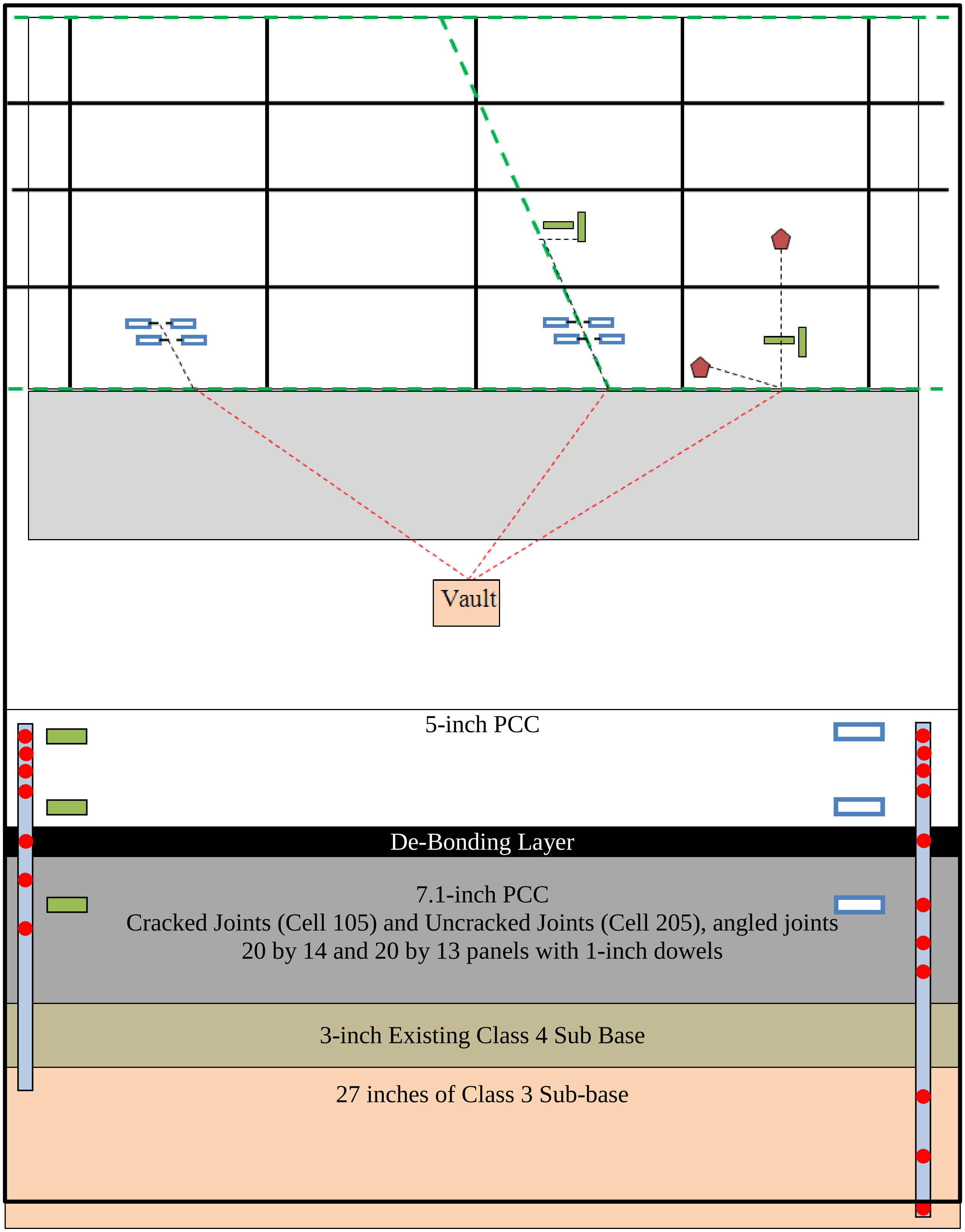

Figure 7: Cell 5 Sensor Layout

Table 11: Cell 5 Sensor Description

Code	Number	Sensor	Description
CE	24	Dynamic Strain	Tokyo Sokki Concrete Embedded Strain Gauge
TC	20	Temperature	Omega Thermocouple Extension Cable, 12 Pair
VW	12	Strain	Geokon, Vibrating Wire Strain Gauge
XV	12	Temperature	Geokon, Vibrating Wire Strain Gauge Thermistor

Surface Texture

Cell 63: Conventional Grind

After repairs, the surface was finished with a conventional Diamond Grind. Prior to Grinding, the contractor observed cell 8 MnROAD and replicated the texture of that cell such that an asperity interval of ½ inch, a groove depth of $^{1}/_{8}$ inch and a groove width of ¼ inch was achieved.

Cell 5: Transverse Boom

Texturing was provided by drawing a broom transversely along the plastic concrete surface. A minimum of 1.2 mm mean profile depth (MPD) behind the paver and a uniformity of 1.2 to 1.5 is the desired setting. The texturing did not proceed until the Engineer certified that texture and geometry lie within this range based on an initial 15-ft run. This was maintained by the acceptable bristle density and uniform pressure. Pictures of the transverse broom surface can be found in appendix C.

Cell 6: Longitudinal Tine

To achieve the best performance the surface was void of bleed water arising from overfinishing or other unacceptable practices.

Prior to texturing to achieve longitudinal tine, an astro turf drag pre-texture was applied. Pretexturing provided a minimum of 1.2 mm mean profile depth (MPD) behind the paver, ahead of the rake bridge. Uniformity of 1.2 to 1.5 mm is the desired setting. Uniform pressure was achieved by the use of a suitable chain providing a uniformly distributed load (UDL). The use of aggregate to achieve the UDL was prohibited. The texturing did not proceed until the engineer certified that texture and geometry based on an initial 15-ft test run lie within this range. This was maintained by the acceptable bristle density and uniform pressure. The surface was void of scrapings. Scrapings that will inhibit subsequent tining are not acceptable.

Texture was achieved with a rake or equivalent device that imprinted sufficient longitudinal tines at acceptable interval to produce a texture to guarantee an MPD of 1.3 to 1.5mm behind the paver. The rake was checked for missing, bent, or broken tines before and during tining. Also check the tine spacing and make sure the tines are clean. Flexible tines cause variability in the spacing of the grooves created in the pavement and thus make it impractical to achieve required groove spacing.

The rake provided pavement grooves of ¾ inch (19 mm) spacing from groove to groove. The tining spacing was perpendicular to the direction of travel. Excessive wander from a path parallel to the centerline was unacceptable. The tining depth was chosen to ensure sufficient friction but shall in no case be less than $^{1}/_{8}$ inch deep. The grooves were $^{1}/_{8}$ inch deep or greater to guarantee an initial smooth tire friction number of 45.

CHAPTER 4: CELL 6 GRADING AND BASE

Laboratory Constant Head Permeability

Laboratory permeability testing was completed by foundation lab personnel and is included as Appendix B. The procedure for this test closely followed ASTM D 2434-68 Standard Test Method for Permeability of Granular Soils (Constant Head). The compaction method chosen was compaction by sliding weight tamper. Additionally, two methods were used to develop flow through the test apparatus. First, the flow was increased by slightly adjusting the outflow valve for seven tests until the valve was fully open. Next, six additional tests were performed in which the flow was increased by raising the hydraulic head in the system.

In Situ Permeability

In situ permeability testing was performed August 17, 2011 at the locations listed in the following table.

Table 12: Permeability Testing

Location	k(cm/s)
sta 1135+25 center lane	8.25E-03
sta 1135+25 center lane	9.77E-03
sta 1135+25 driving lane right wheel path	3.02E-03
sta 1135+75 center lane	1.55E-02
sta 1135+75 center lane	1.93E-02
sta 1135+75 driving lane right wheel path	1.43E-04
sta 1135+75 driving lane right wheel path	9.27E-04

Note: Wet base, bathtub condition in outer portion of lane

In Situ Performance Based Construction Quality Assurance Testing

In situ quality assurance testing was performed August 17, 2011 using the dynamic cone penetrometer (DCP) and light weight deflectometer (LWD). A brief introduction to the DCP and LWD is provided below. Because there is some ambiguity regarding the terminology applied to quality assurance testing and mechanistic pavement design, definitions of the following terms are also provided here (Newcomb and Birgisson, 1999).

• *Elastic Modulus* – The applied axial stress divided by the resulting axial strain within the linear range of stress-strain behavior of a material.

• *Resilient Modulus* – The stress generated by an impulse load divided by the resulting recoverable strain after loading.

• *Modulus of Subgrade Reaction* – The applied stress imposed by a loaded plate of a specified dimension acting on a soil mass divided by the displacement of the plate within the linear portion of the stress-deformation curve.

• *Stiffness* – A qualitative term meaning a general resistance to deformation. It is often used interchangeably with elastic modulus, modulus of subgrade reaction, and resilient modulus. It largely determines the strains and displacements of the subgrade as it is loaded and unloaded.

• *Shear Strength* – A combination of a material's interparticle friction and its cohesion in resisting deformation from an applied stress. This is the largest stress that the material can sustain.

DCP Background

MnDOT implemented an aggregate base quality assurance specification for the DCP in 1998. The DCP's falling mass drops from a specified height to drive the cone into the pavement foundation material. The DCP penetration distance per drop is known as the DCP penetration index (DPI). The DPI can be used to estimate the shear strength and modulus of unbound materials using empirical relationships. The original DCP specification was designed for use on aggregate base. That specification was later modified to take gradation and moisture effects into account in order to increase its accuracy and expand its application to other granular materials. Both the grading number and moisture content have a strong influence on the DPI, and therefore, target DPI values are determined according to a soil's grading number and moisture content (Oman, 2004).

LWD Background

The portable LWD, (ASTM E 2583–07, Standard Test Method for Measuring Deflections with a Light Weight Deflectometer) and (ASTM E 2835–11, Standard Test Method for Measuring Deflections using a Portable Impulse Plate Load Test Device), consists of a falling mass (typically 10 kg), an accelerometer or geophone, and a data collection unit. LWDs are designed to be light enough to be moved and operated by one person and are often used to spot check unbound material compaction (Fleming et al., 2007, Mooney et al., 2008, Siekmeier et al, 2009, and White et al., 2007, 2009). LWD quality assurance procedures offer several advantages over the specified density method. On a practical level, the LWD takes less time, is more intuitive, and is able to accurately test more material types. For example, large aggregate creates problems for other tests. In addition, LWD testing is safer because the inspector is able to remain standing and visible during most of the testing process (Davich et al., 2006).

DCP Equipment

The structure of the DCP consists of two vertical shafts connected to each other at the anvil (ASTM D 6951-03). The upper shaft has a handle and hammer. The handle is used to provide a standard drop height of 575 mm (22.6 in) for the hammer as well as a way for the operator to easily hold the DCP vertical. The hammer is 8 kg (17.6 lb) and provides a constant impact force. The lower shaft has an anvil at the top and a pointed cone on the bottom. When the hammer is dropped and hits the anvil, the cone is driven into the ground. Photos of the DCP are shown in the following figure.

Figure 8: Photos of the Dynamic Cone Penetrometer

There are several options available for the DCP, which include different hammer masses, tip type, and recording method. For pavement applications, the 8 kg mass is used because of the highly compacted soil. The DCP tip can either be a reusable hardened point or a disposable cone. The reusable hardened point stays on the DCP for an extended period of time, until damaged or worn beyond a defined tolerance, and then replaced. The disposable cone remains in the soil after every test, making it easier to remove the DCP. Manual or automated methods are available to record penetration measurements. The reference ruler can be attached or unattached to the DCP. The automated ruler provides equivalent results, but allows a single operator to record the penetration for each drop of the hammer and directly transfer data to other computing devices.

LWD Equipment

There are several types of LWDs and the following is a general description of the LWD shown in the figure below. Moving from top to bottom, the handle is used to keep the shaft vertical. Next along the shaft is a release trigger, which holds the mass in place prior to drop, thereby ensuring a standard drop height and repeatable impact force. Buffers, made of either rubber pads or steel springs, catch the falling mass and transfer the impact force to the loading plate. Below the buffers is a measurement device that measures the deflection, and the force for some models. At the bottom is the loading plate, which must be in full contact with the ground.

Figure 9: Light-Weight Deflectometer

Seven LWD models have been used in Minnesota and there are a variety of differences between these devices. MnDOT currently supports only the ZFG 2000 for quality assurance in order to achieve measurement consistency state-wide. Measurement differences are caused by several factors. LWDs can have a fixed drop height, while others have adjustable drop heights. Some measure deflection using an accelerometer fixed inside the load plate, while others use a geophone that passes through a hole on the bottom of the plate to directly contact the surface. Some LWDs assume a peak load established during trial testing, while others include a load cell. Finally, the buffer and plate stiffness affect how the energy of the falling mass is transferred to the ground (Mooney and Miller, 2009 and Vennapusa and White, 2009). Due to all these factors as well as other considerations, MnDOT has elected to support only one LWD model for quality assurance testing.

DCP Test Procedure

The DCP test procedure is currently standardized by both ASTM D 6951-03 and the MnDOT Grading and Base Manual. The following is a brief description of the test procedure used during this project. First, the equipment was inspected for any fatigue or damaged parts, and that all connections were securely tightened. The operator holds the DCP vertical, lifts the hammer from the anvil to the handle, and then releases the hammer. A second person records the height at the bottom of the anvil in reference to the ground and then records the new height after each drop.

Small penetration rates represent better compaction. The current methods of compacting pavement foundation material involve building thin individually compacted layers less than 12 inches (30 cm). This causes the material closer to the surface to be less confined and less compacted then the deeper material. Therefore, deeper DCP measurements should typically show increased strength due to increased confinement.

LWD Test Procedure

LWD devices are configured and used differently depending on the model and the testing agency (ASTM E 2583–07, Standard Test Method for Measuring Deflections with a Light Weight Deflectometer) and (ASTM E 2835–11, Standard Test Method for Measuring Deflections using a Portable Impulse Plate Load Test Device). A brief summary to of the general procedure is provided here.

Prior to placing the LWD on the material to be tested, the surface is leveled. Particularly loose or rutted surface material is removed to a depth of about 15 cm. Three seating drops are performed prior to data collection to ensure that plastic deformation of the surface material does not affect the measurements. Once the LWD has been seated, the data collection should consist of three measurement drops. The three values resulting from these measurement drops are averaged to create one mean value for that test location. The operator will often notice that the modulus values increase slightly during the three measurement drops from a fixed height. If this increase exceeds 10 percent it is probable that the material has not been adequately compacted. Reliable measurement values cannot be obtained until the material has been corrected.

LWD devices should not be used when the temperature falls below 5 degrees Celsius (41 degrees Fahrenheit) to ensure that the device’s components, particularly the rubber buffers, work as intended. There is no practical upper limit on the temperature. While most LWDs will work in the rain, it should be noted that moisture greatly affects the strength and stiffness characteristics of the unbound materials. It is necessary to measure the moisture content in conjunction with every test using an in situ moisture testing device or by removing a sample for an oven-dry test.

When control strips are used to verify the LWD target value, it is important that the layer structure of the control strip is considered. This is because deeper layers within the pavement foundation can affect LWD measurements even though the primary depth of influence is close to the plate diameter.

In the case of Zorn LWDs, the applied force from the falling mass is measured at the factory and used for all future modulus calculations for that particular LWD. The following equation can be used to estimate the applied load for Zorn LWDs.

$$F_Z = \sqrt{2 \times m \times g \times h \times k}$$

where:

F_Z	=	estimated force [N]
m	=	mass of falling weight [kg]
g	=	acceleration due to gravity [9.81 m/s^2]
h	=	drop height [m]
k	=	spring constant [362396.2 N/m]

Other LWDs include a load cell to measure the load and then combine this load with the deflection to estimate the modulus for each drop. Although it is inevitable that the applied force will not be the same for materials of different stiffnesses, White reported that the "assumption of constant applied force does not lead to significant variations in the estimated modulus" (White *et. al.*, 2007). Another factor that affects the estimated modulus in all LWDs is the plate size. The following equations show the commonly used calculations used to estimate the modulus.

$$E_{LWD} = 2r_p\sigma(1-\nu^2)\frac{(1\times10^6)R}{\Delta}$$

$$\sigma = \frac{F}{1000\pi r_p^2}$$

where:

E_{LWD}	=	Young's modulus [MPa]
r_p	=	plate radius [m]
σ	=	peak stress applied to the soil [MPa]
ν	=	Poisson's ratio of the soil
R	=	plate rigidity (0.79 for rigid, 1.0 for flexible)
Δ	=	peak soil deflection [μm]
F	=	peak force applied to the soil [kN]

As previously stated, Zorn LWDs use a steel spring buffer and an accelerometer embedded in the plate, combined with double integration, to measure deflection. Other LWD models use rubber buffers and a geophone in contact with the ground, combined with single integration, to measure deflection. Previous studies have found that Dynatest/Keros moduli were about 1.75 times greater than Zorn moduli when the drop height, mass, and plate size were constant (White *et. al.*, 2007).

A previous study completed by MnDOT recommended standardizing the LWD mass at 10 kg (22.0 lb), the drop height at 50 cm (19.7 in), and the plate diameter at 20 cm (7.9 in) for ease of use and in order to have an appropriate influence depth to test for a lift of compacted pavement foundation material (Davich *et al.*, 2006). Plate size affects the measurement depth, confinement, and stress level applied to stress dependent materials. Standardizing the LWD plate size to 20 cm reduces these variables and allows the target modulus to be estimated. Because the buffer type affects the force delivered to the ground, MnDOT now specifies that a force of 6.28 kN be delivered to the ground. This equates to a stress of 0.2 MPa for a 20 cm diameter plate. LWD tests in Minnesota are currently conducted using that configuration, along with the test guidelines and advice contained in the manufacturer's literature.

DCP and LWD Measurements

Table 13: DCP and LWD Measurements

Location (station)	DPI (mm/drop)	LWD (mm)	Moisture (%)
113675	11	0.90	7.1
113676	14	0.73	5.4
113625	14	1.09	8.2
113626	14	0.89	na
113575	16	0.86	7.2
113576	11	0.93	7.3
113525	17	0.74	6.9
113526	16	0.97	6.0
113475	12	0.67	7.2
113476	10	0.63	6.4
113425	27	0.68	7.4
113426	12	1.90	6.8
113375	23	0.83	7.7
113376	15	0.65	6.7
113325	14	0.83	7.6
113326	13	0.66	8.2
113275	15	1.66	7.0
113276	16	1.09	na
113225	19	1.10	5.6
113226	12	1.35	7.4

DCP, LWD and Moisture Summary

The DCP, LWD and moisture measurements are plotted in the figure below. In summary, it appears that the OBAG Special in test section 6 is reasonably uniform except near the west end and near station 1134+25. In general, the LWD deflections and DCP penetration (converted to a deflection estimate) are similar to past MnROAD measurements for similar layer geometries.

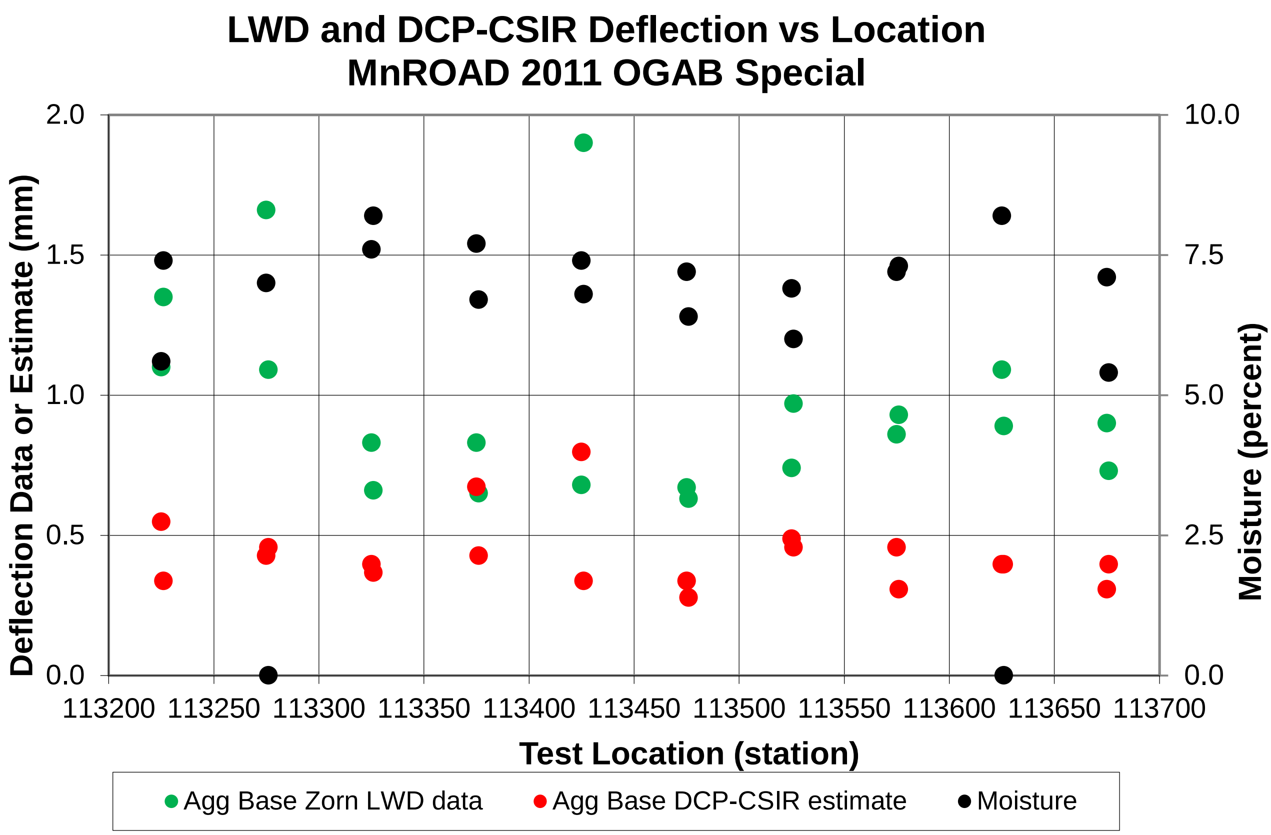

Figure 10: LWD and DCP-CSIR Deflection vs. Location

Grain Size Measurements

The grain size measurements in the following figure show that the OGAB special is coarser than typical MnDOT Class 5 aggregate.

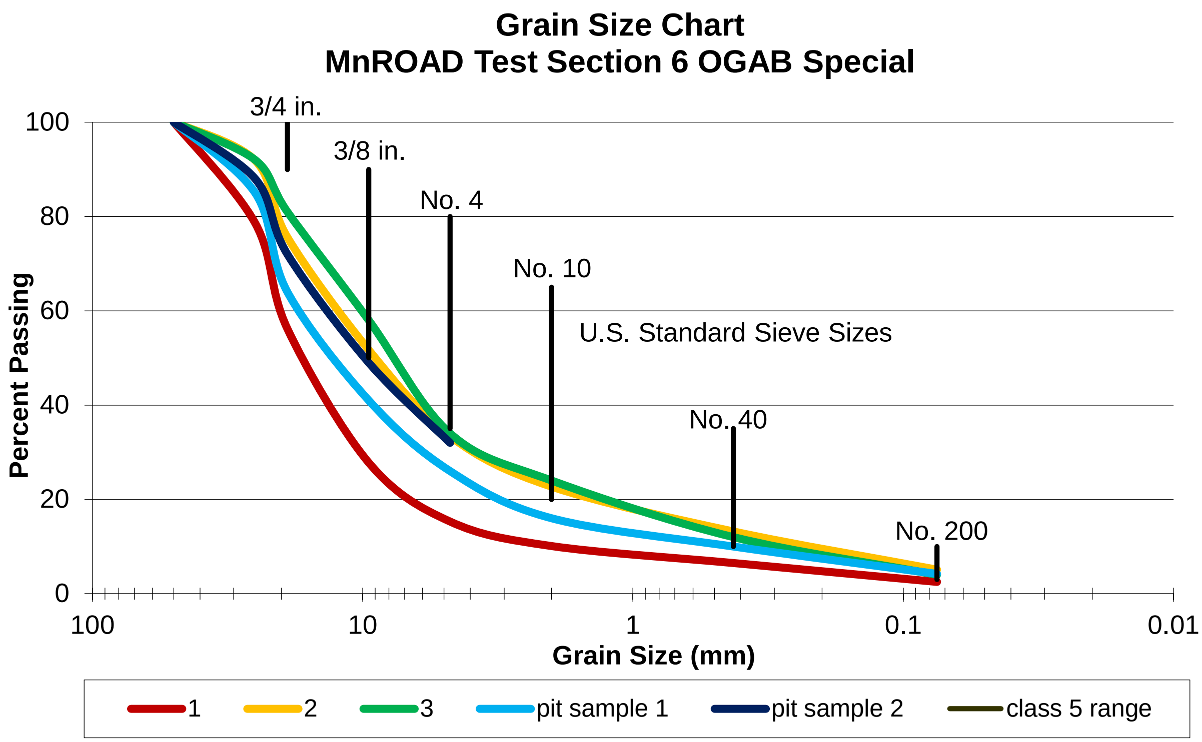

Figure 11: Grain Size Chart MnROAD Test Section 6 OGAB Special

CHAPTER 5: CONSTRUCTION SEQUENCE

The MnDOT field staff of Golden Valley, including a host of surveyors, inspectors, and other administrative staff, were responsible for the construction administration for the project. It was let as SP8680-165. CS McCrossan was awarded the contract for their low bid of $469,592,

MnROAD staff completed forensic activities on Cells 5 and 6 before they were removed. These activities included coring along longitudinal and transverse joints to investigate their condition and coring out sensors to determine their position and orientation. Forensic activities were completed Monday, August 1, 2011.

Figure 12: Cell 5 before Reconstruction

Figure 13: Cell 5 Stripping of PASSRC

The contractor began construction activities on Monday, August 1 with removals in Cell 5. The PASSRC layer proved to be an easy removal by remaining adhered to the top concrete layer. In fact, the stripping from the old concrete layer beneath the PASSRC was visible.

Next, the panel removals in cell 63 began, shown in the photograph below.

Figure 14: Cell 63 Panel Removals

Sensors were then installed in Cell 5 and the pavement removal began in Cell 6.

By August 4th, the contractor finished removals of all the panels in Cell 63. By August 5th, removal in Cell 6 was complete, all removals areas in cell 63 were cleaned, and a rough grade of cell 6 was completed to allow drainage over the weekend.

Figure 15: Cell 63 Tar Paper over Bituminous Crack

After the weekend storm, the contractor's crew were onsite on August 9, 2011 to clean the debris and standing water out of the areas scheduled for replacement. Cleaning was completed using an air compressor. MnDOT placed tar paper over the top of the crack in the existing bituminous pavement to reduce reflective cracking in the new concrete. A 6" piece of felt was placed whereever there was a longitudinal crack in an adjacent panel to the new panel. Concrete arrived from Aggregate Industries later that day to pour in the panels. The first truck onsite was rejected do to high slump and air. A total of 5 trucks were onsite this day. Concrete placement was completed at approximatly 4:00 p.m. After placement sawing of the concrete was completed.

Figure 16: Cell 63 Concrete Panel Replacement

Construction activities for Cell 6 also continued on August 9th with a stringline set for grading the subgrade and base. Cell 6 was excavated to subgrade level. The old Class 5 material was hauled and stockpiled in the MnROAD stockpile area.

At this point, MnROAD staff completed instrumentation needed on Cell 5 prior to fabric placement. They also completed the initial instrumentation in the subgrade of Cell 6.

Figure 17: Cell 5 Instrumentation Prior to Fabric

The OGAB special for Cell 6 was placed on August 16, and completed on August 17. It is beneficial to note that the night of August 16th, MnROAD received approximatly a 2-inch rainfall and several people observed the rain water flowing from the OGAB special base into the drains excavated in the shoulders by the contractor. Base material remained firm even after the rain event. MnDOT researchers were onsite on the 17th to perform tests on the OGAB special. They performed field permeablity testing, Light Weight Deflectometer (LWD) testing, Dynamic Cone Pentrometer (DCP) testing, and took moisture samples from the areas tested. Sensor installation was then completed and data collection began. On August 18, McCrossan's crews preped and placed the OGAB special material in the stock pile area in preparation for the Roller Compacted Concrete (RCC) Demonstration Slab. Dowels were set in Cell 6 on August 19, in preparation for the paving scheduled for August 22.

Figure 18: Cell 6 OGAB Special Placement

Figure 19: Cell 6 OGAB Special DCP Testing

Fabric was delivered onsite and ready for placement for Cell 5.

Cell 6 was paved on Monday, August 22. Paving began around 8:45 am and was completed in this cell around 1:30 p.m.

Figure 20: Cell 6 Sample Preperation

Figure 21: Cell 6 Paving

Figure 22: Cell 6 Construction

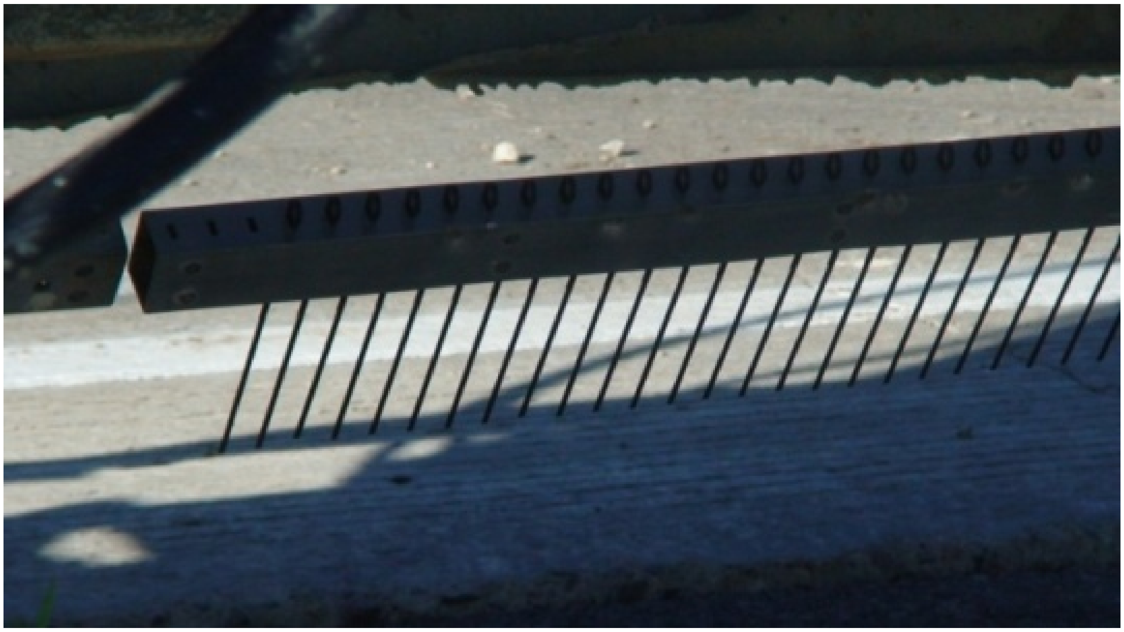

Figure 23: Cell 6 Longitudinal Tining Equipment

Figure 24: Cell 5 Turf Drag Before Tining

After the concrete paving was complete on August 22, the contractor installed the fabric on Cell 5. MnROAD staff installed the sensors on Cell 5 on Tuesday, August 23. Cell 5 was paved on Wedensday morning beginning around 8:30 a.m.

Figure 25: Cell 5 Fabric and Dowel Placement

Figure 26: Cell 5 Finishing

The Roller Compacted Concrete (RCC) Demonstration slab was paved on Friday, August 26.

Figure 27: Demo Slab Paving

Figure 28: Demo Slab Lift Thickness

Figure 29: Demo Slab

Figure 30: Demo Slab Compaction

Figure 31: Demo Slab Density Testing

Work continued on the Mainline Cells 5 and 6 with C.S. McCrossan preparing the shoulders August 30th and 31st . By September 1st, C.S. McCrossan began hauling the OGAB special material and placing. The Contractor also fine graded and compacted the material in preparation of placement of the RCC shoulders.

Paving of the RCC shoulders was on Friday, September 2, 2011. Paving began at 8:00 a.m. and continued until about 3:00 p.m. Material was placed on the outside shoulder using a bituminous paver and on the inside shoulder using a shouldering machine. Joints were sawed in half of both Cells 5 and 6 shortly after completion of paving.

Figure 32: RCC Shoulder First Passing Lane

Figure 33: RCC Shoulder Second Driving Lane

Figure 34: RCC Shoulder Compaction

Table 13 is a summary of MnDOT's field notes taken during reconstruction. The notes reflect the main activities by the contractors that occurred each day.

Table 14: Field Construction Notes/ Daily Summary

Date	Notes
8/1	C.S. McCossan began to layout the silt fence. They began removals of existing concrete and PASSRC in cells 105 and 205. Concrete panels scheduled for removal in Cells 60-63 were marked for removals.
8/2	The removals in cells 105 and 205 were completed. Panel removals were started in cells 60-63.
8/3	MnROAD staff began sensor installation in cells 105 and 205. Contractor began removals in cell 6 and continued panel removals in cells 60-63.
8/4	Contractor finished panel removals in cells 60-63. MnROAD staff installed some rebar into a few repairs in cell 63. Removals in cell 6 were completed.
8/5	MnROAD staff began to install sensors in cell 6. A weekly construction progress meeting held onsite.
8/9	Contractor placed concrete in the panel repairs in cell 60-63. Sawing of the joints was also completed.
8/16	MnROAD staff completed sensor installation in the subgrade of cell 6. Contractor finished grading the subgrade of cell 6 and began hauling the OGAB special base aggregate. The contractor cut some drains into the shoulders to allow drainage from the OGAB special because rain was expected overnight. 4 of 12 sensor trees were installed before the rain began.
8/17	The OGAB special base aggregate seemed to be free draining after the rainfall encountered overnight. The Contractor finished grading the base. MnROAD staff completed installation of the sensors in cell 6. MnDOT research staff performed several tests on the OGAB special base. These tests included permeability, LWD, and DCP.
8/18	The Contractor began prepping the roller compacted concrete (RCC) demonstration slab in the MnROAD stockpile area.
8/19	Weekly construction progress meeting held onsite. The Contractor placed dowel baskets and installed dowels in the headers of cell 6.
8/22	Cell 6 was paved beginning at 8:45 am and finishing about 2:00 p.m. The joints were cut into the pavement. C.S. McCrossan placed the geotextile interlayer on cell 5 beginning about 2:30 p.m.
8/23	The contractor was onsite preparing the paver for paving of cell 5. Tie bars on baskets were also installed in preparation to paving. MnROAD staff completed sensor installation in cell 5.
8/24	Paving began onsite at 8:15 a.m. and was completed around 11:15 a.m. Joints were sawed shortly afterwards. The contractor was onsite placing grade stakes for the shoulders in cell 6.
8/26	Weekly construction progress meeting held onsite. Then the contractor paved the RCC demonstration slab. Joints were cut into the first 100’ of the slab.
8/29	RCC in demonstration area was noted to have check cracking appearance. Concerns were expressed to contractor about moving forward with paving on the Mainline.
8/30	C.S. McCrossan began prepping the shoulders with in cell 6.
8/31	C.S. McCrossan continued prepping shoulders. Met onsite with C.S. McCrossan to discuss the finish RCC in demo area. Currently there is a lot of check like cracking in the surface that is a concern. C.S. McCossan will look into their mix and make a few adjustments before paving shoulders on the Mainline. Moving forward with RCC paving tomorrow.
9/1	OGAB special was hauled and placed in cell 6. First truck arrived onsite at 8:15 a.m.
9/2	RCC shoulders paved on cells 6 and 5. First truck arrived at 8:00 a.m. Contractor used an asphalt paver on the outside shoulders and a shouldering machine on the inside shoulders. Smaller rollers were used instead of the large ones in the demonstration slab. Overall appearance was better than the demonstration slab. Some check cracking was still present.

Initial Plastic Concrete Results

Plastic concrete tests were performed on the fresh concrete for all three cells. Slump, air, and temperature were measured at different times throughout paving. The results are listed in the table below.

Table 15: Cell 63 Plastic Test Results

Cell 63		
Batch 1 (Rejected)		
Slump	4.5	in
Air	9.1, 9.0	%
Batch 2		
Slump	1.75	in
Air	6.9	%

Table 16: Cell 6 Plastic Test Results

Cell 6		
Inspector (8:45 am)		
Slump	1.5	in
Air	6.5	%
Start (8:52 am)		
Slump	0.5	in
Air	7.1	%
2nd or 3rd Batch		
Slump	2.75	in
Air	7.4	%

Table 17: Cell 5 Plastic Test Results

Cell 5		
Batch 1 (AM)		
Slump	2	in
Air	6.2	%
Temp	81	degrees

CHAPTER 6: EARLY PERFORMANCE EVALUATION

Both laboratory and field tests were performed to assess the initial performance of the newly constructed test cells.

In the following plots and text, Cell 5 refers to sections 505 and 605 together and Cell 6 refers to sections 306 and 406 together, unless otherwise noted. For some surface characteristic tests, cell 305 and 405 must also be included in measurements for Cell 5.

Strength

Strength testing was performed at the MnDOT Office of Materials and Road Research Laboratory. Both compressive and flexural strength tests were measured on sample specimens prepared during construction using material sampled from the batches used for paving. The specimens were allowed cure on site and were then transported back to the lab after initial hardening.

Compressive Strength

Compressive strength samples for the RCC concrete were prepared using ASTM Standard C1435, “Standard Practice for Molding Roller-Compacted Concrete in Cylinder Molds Using a Vibrating Hammer.” This standard requires a tamping plate be attached to vibrating hammer which is used to compact the concrete cylinder in two separate lifts. Compressive strength was tested according to the ASTM C39, standard test method using molded cylindrical specimens.

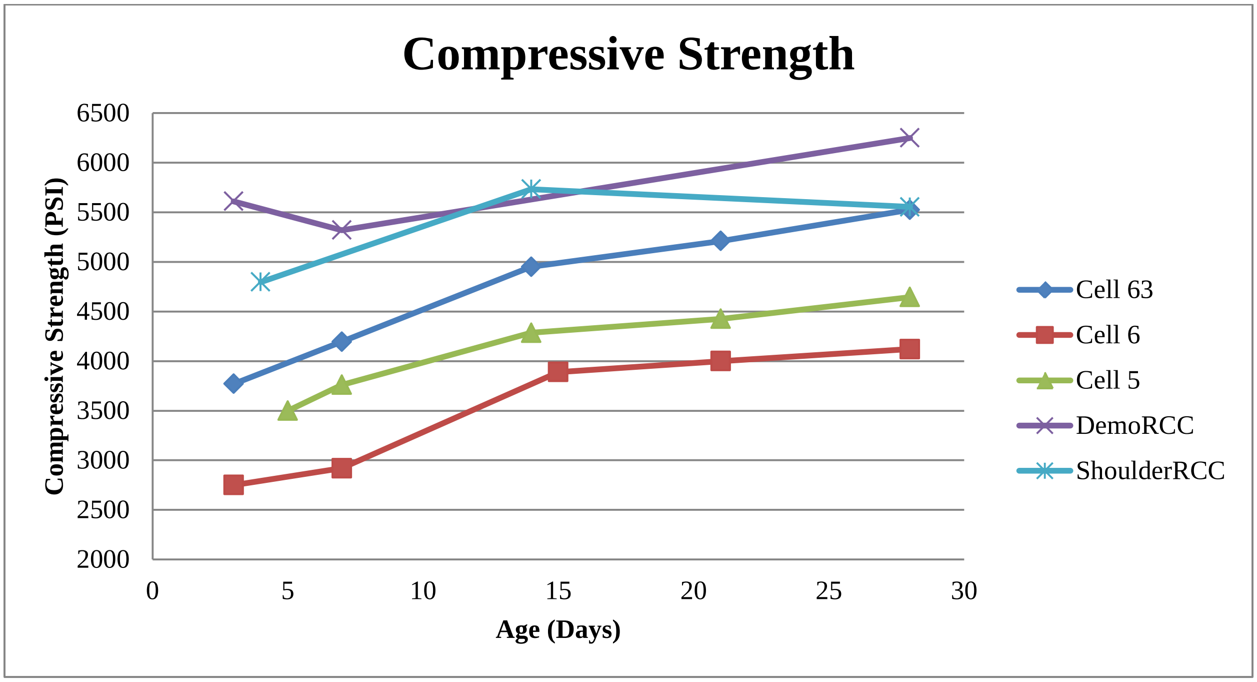

Figure 35: Compressive Strength Results

As is seen in this plot, the RCC for both the demo and shoulders of cells 5 and 6 had the highest compressive strength. The RCC does not show as much strength gain as the other three cells, but started with much higher initial strength. The repair material used in Cell 63 had higher strength than both Cells 5 and 6.

Flexural Strength

Because there is no standard for preparing flexural strength specimens using roller compacted concrete, a method of compaction was used which mimics that of the compressive strength standard. A tamping plate was designed to fit within the beam molds and cover the entire surface. This plate was then attached to a vibrating hammer. Beams were prepared using both one lift followed by compacting, and with two lifts each followed by compaction. The specimens were tested for flexural strength according to ASTM C78, standard test method for flexural strength of concrete using a simple beam with third-point loading. The results are shown in the plots below.

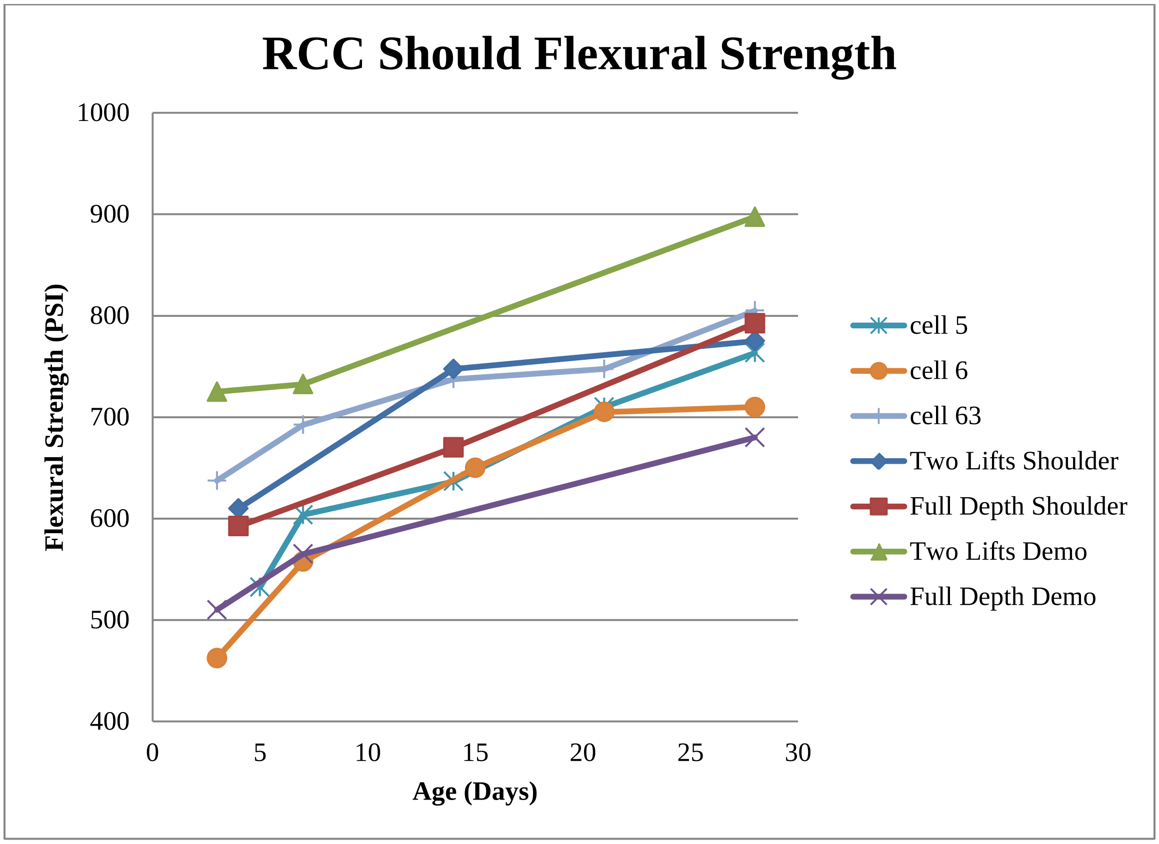

Figure 36: Flexural Strength Results

Interestingly, from this plot you can see that the preparation method used for the RCC specimens greatly impacts the flexural strength. The beams prepared in two lifts of RCC during the demo slab construction had the highest final strength of all cells, while the beams prepared with just one lift also from the demo slab have the lowest final strength. This suggests the amount of compaction/lifts done during construction of RCC pavements will greatly influence the strength. Again, the repair material in Cell 63 had higher flexural strength than the concrete used in the full-depth Cells 5 and 6. There was little difference in flexural strength between Cells 5 and 6.

Ride Quality

The International Ride Index (IRI) is measured using two different pieces of equipment mounted on the Lightweight Inertial Surface Analyzer (LISA). The LISA shown in the figure below is a profile device used to measure the amount of vertical rise over a horizontal distance. This is done with two separate laser sources on the side of the vehicle: The Roline laser which takes continuous profile measurements over a 4-inch path, and the TriODS laser which measures three discrete profiles across the 4-inch path. The raw data collected from these lasers is then used to calculate two different IRI values. This is done with a mathematical simulation that estimates the amount of vertical movement a vehicle would experience while driving. The simulation uses a higher IRI to correspond to a rougher pavement. It is important to note that the calculated IRI can be highly dependent on the section length; a single rough spot would have a larger negative influence on a shorter segment than it would on a longer one.

Figure 37: Light Weight Profiler Equipment with Roline and TriODS

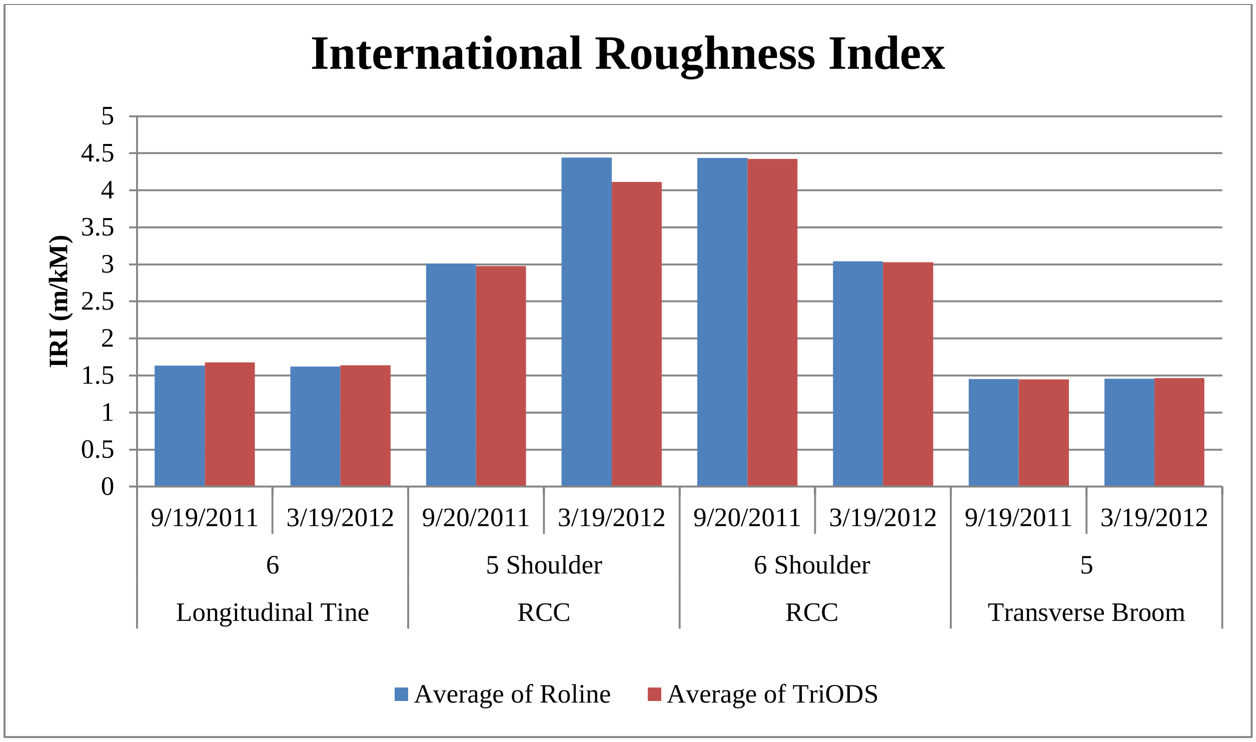

Figure 38: International Roughness Index Results

As you can see from this chart, IRI in cells 5 and 6 does not significantly change from right after construction to the following spring. The RCC shoulders have significantly higher IRI than the longitudinal tine and transverse broom. The longitudinal tine is only slightly higher in IRI than the transverse broom.

On-Board Sound Intensity

The On-Board Sound Intensity (OBSI) test measures the noise generated from the tire interaction with the pavement surface (AASHTO TP 76-09) . The test is performed while driving at freeways speeds, when the dominant noise generation source becomes that from the tire-pavement interaction. One benefit of OBSI testing is that it allows noise generated from the pavement-tire interaction to be isolated from other sources, such as engine noise. OBSI is also not subject to influence from other landscape and surrounding environmental factors, making it favored to the traditional Statistical Pass By Method. The tire-pavement interaction noise is measured using four intensity meters mounted on the tire near the pavement surface. This setup is shown in the figure below. The sound intensity captured from these meters is then used to calculate OBSI using following logarithmically scaled, A-weighted equation to closely relate it to the human hearing spectrum.

$$OBSI = 10\log_{10}\left[\sum_{i=1}^{n} 10^{(SI_i/10)}\right]$$

$$i = Third - Octave\ Frequcny$$

$$SI_i = Measured\ Sound\ Intensity\ at\ frequency\ "i"$$

The OBSI is determined by averaging the sound intensity measurements from each of the following 12 third-octave frequencies: 400, 500, 630, 800, 1000, 1250, 1600, 2000, 2500, 3150, 4000, and 5000 hertz.

Figure 39: On-Board Sound Intensity Meters

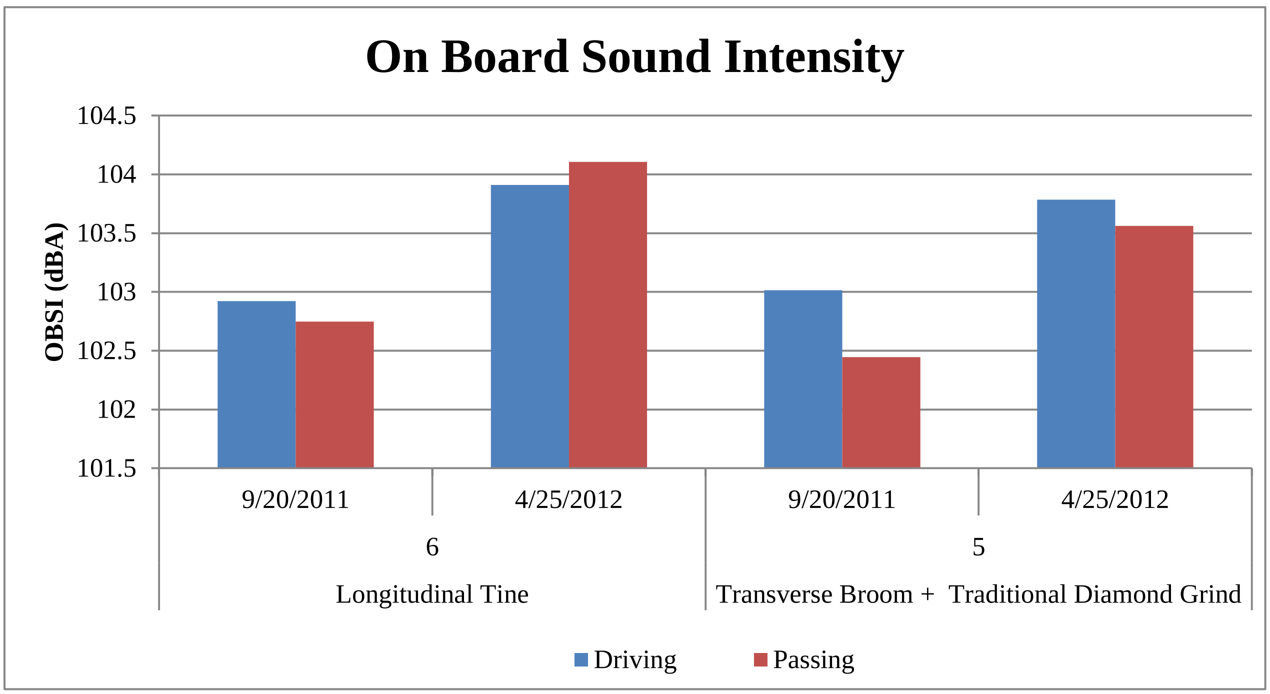

Figure 40: OBSI Results

Because of the length required for this test, the new test sections in Cell 5 (505 and 605) were measured with the old diamond grind sections in Cell 5 (305 and 405), so the resulting OBSI is from a combination of both surface textures. You can see from this chart that the OBSI was much higher in the spring than fall for both cells. Immediately after construction, the OBSI of the longitudinal tine in cell 6 was less than the transverse broom and diamond grind in Cell 5, however this trend was opposite in the spring.

Friction Number

Cell 5 and 6 were tested for friction with the standard method used at MnROAD. This method utilizes the KJ Law Friction Trailer show in Figure 41to perform skid testing of the pavement surface. This test is usually performed twice annually on all cells at MnROAD. Friction testing is done in accordance with the following three ASTM standards for skid resistance of paved surfaces: ASTM E274 using a full-scale tire, ASTM E501 using a standard ribbed tire, and ASTM E524 using a smooth tire. The friction trailer is pulled at 40 mph speed. Once the trailer mists the pavement surface with water, a break activates locking the wheel in place. This applies both horizontal drag forces and vertical load forces to the pavement. Sensors located at the wheel assembly take the friction measurements. The test is performed on both wheel paths and in both lanes. The ribbed tire is tested in the left wheel path, and the smooth tire is tested in the right wheel path. The test generates friction numbers between 0 and 100. A pavement with a friction number from a smooth tire of 25 is considered a safe pavement with adequate skid resistance. A friction number less than 15, however, would describe a pavement needing rehabilitation to achieve sufficient skid resistance [1].

Figure 41: Friction Trailer

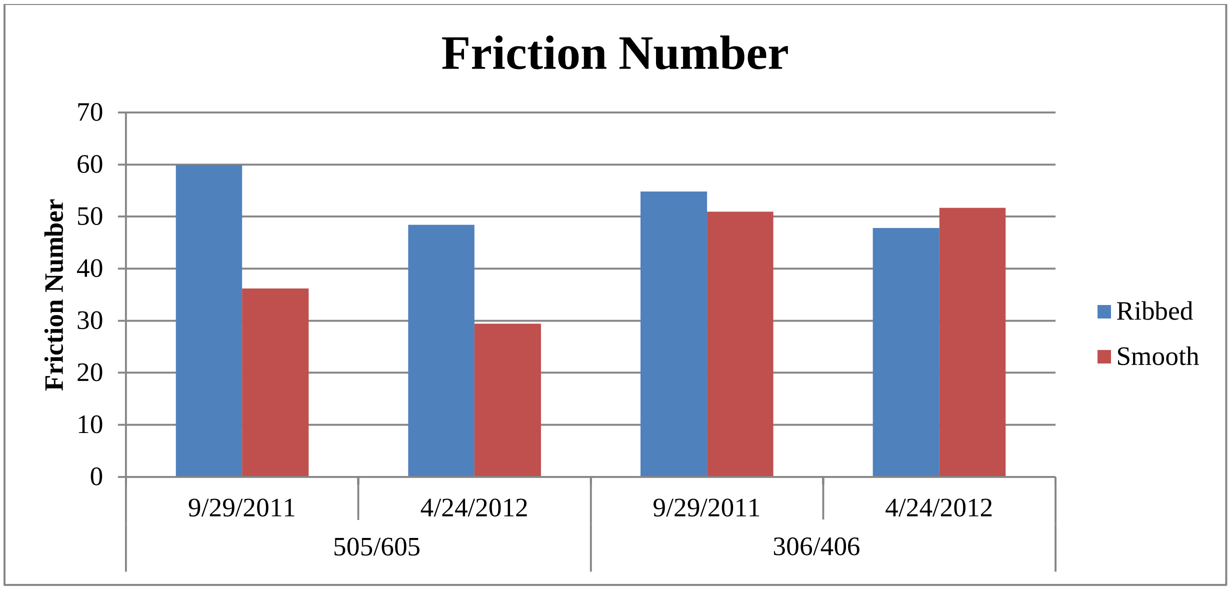

Figure 42: Friction Number Results

The friction number for both test cells was slightly lower in the spring than in the fall right after construction. The longitudinal tine in Cell 6 generally had a higher friction number than in Cell 5.

Surface Texture

To analyze the surface of Cells 5 and 6, a Circular Texture Meter (CTM) was used to measure the profile of the pavement surface. The CTM shown in figure 43 below is used in accordance with ASTM E2157. The texture meter uses a laser to measure the profile depth throughout an 11.2-inch diameter circle. This profile is segmented into eight sections, and the average of the mean profile depth for each segment is calculated. The test is performed three times at each location, and the root mean square of all tests is taken as the final mean profile depth.

Figure 43: Circular Track Meter

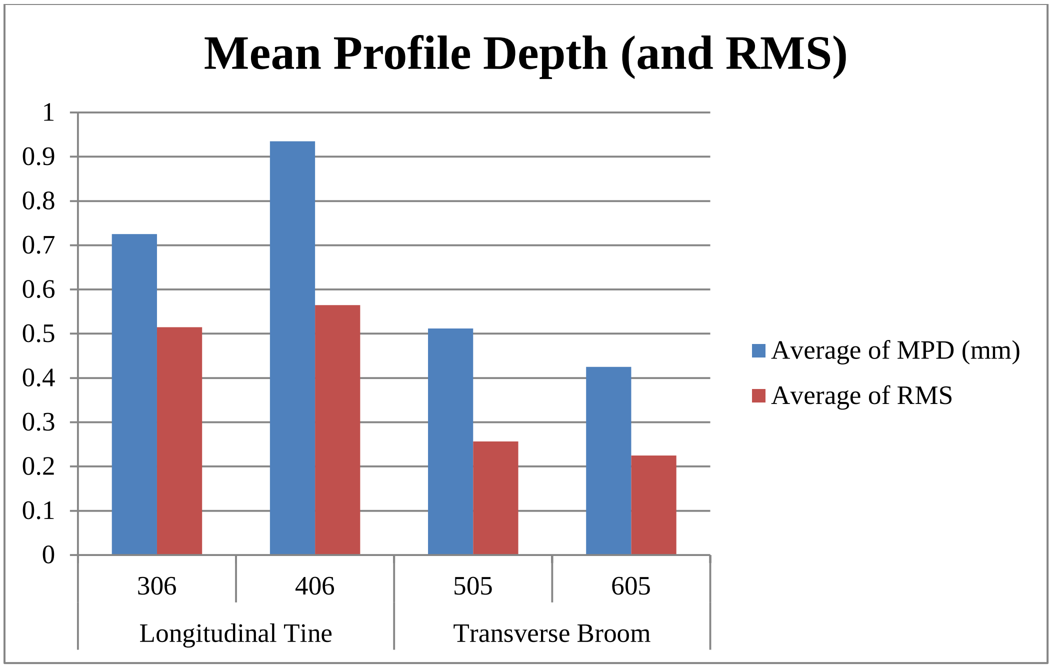

Figure 44: CTM Results

The transverse broom in Cell 5 has a lower MPD than the longitudinal tine in Cell 6. There is variation between the subsections of each cell, which suggests some inconsistency in paving.

Nuclear Density

The density of the RCC throughout construction the demo slab was measured using the Seaman C-200 Nuclear Density Test device in figure 45. This device allows for very fast, non-destructive, in field measurements of densities ranging from 70 to 170 pounds per cubic foot. The Nuclear Density Gauge has an internal radioactive source that emits a known amount of gamma radiation to the pavement surface. Some radiation is absorbed into the pavement, while the radiation that gets reflected is measured by a Geiger-Muller detector tube. The detector measures the electrical pulses from the ionized gasses created from the reflected radiation. This meter count is then used to estimate the density of the pavement.

Figure 45: Nuclear Density Meter

Density measurements were taken immediately after placement (uncompacted) and again after each pass of the drum rollers for each load. From the plot below, it is clear that there is a large increase in density with the first pass of compaction. However, this increase becomes much less in the second pass. By the third pass, the density generally decreased.

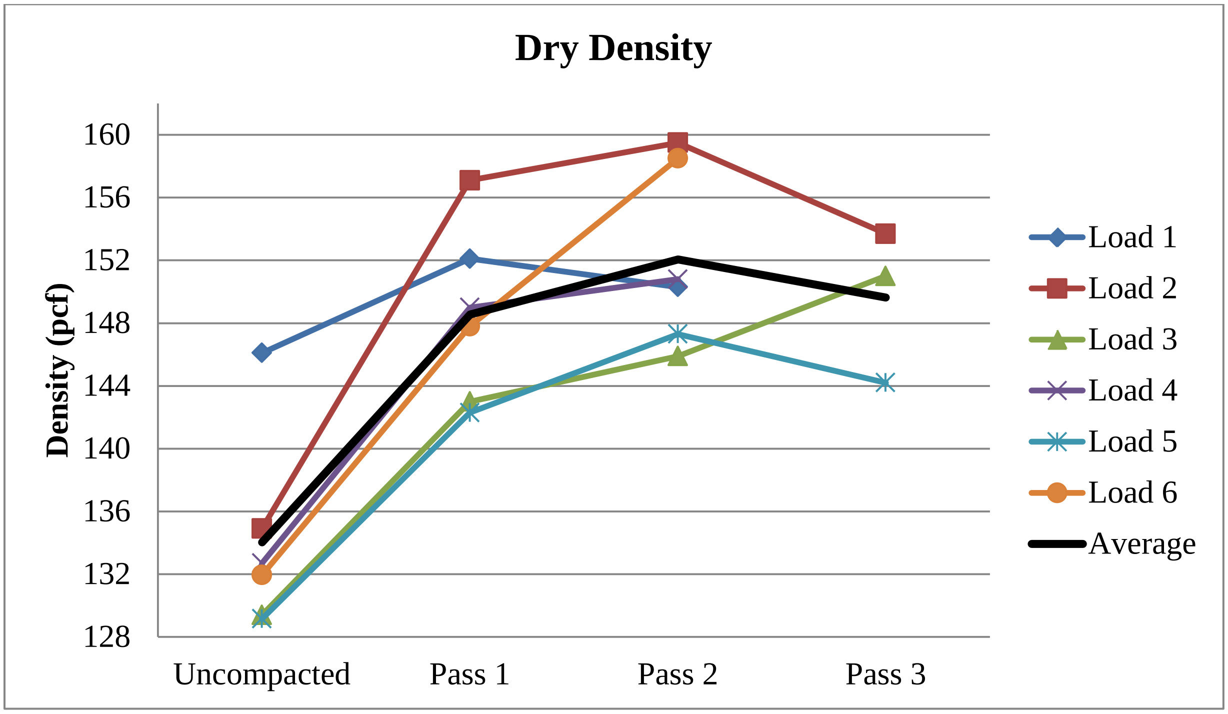

Figure 46: RCC Density Results

The trend for moisture is not as clear as it is for density. The trend was highly dependent on the load.

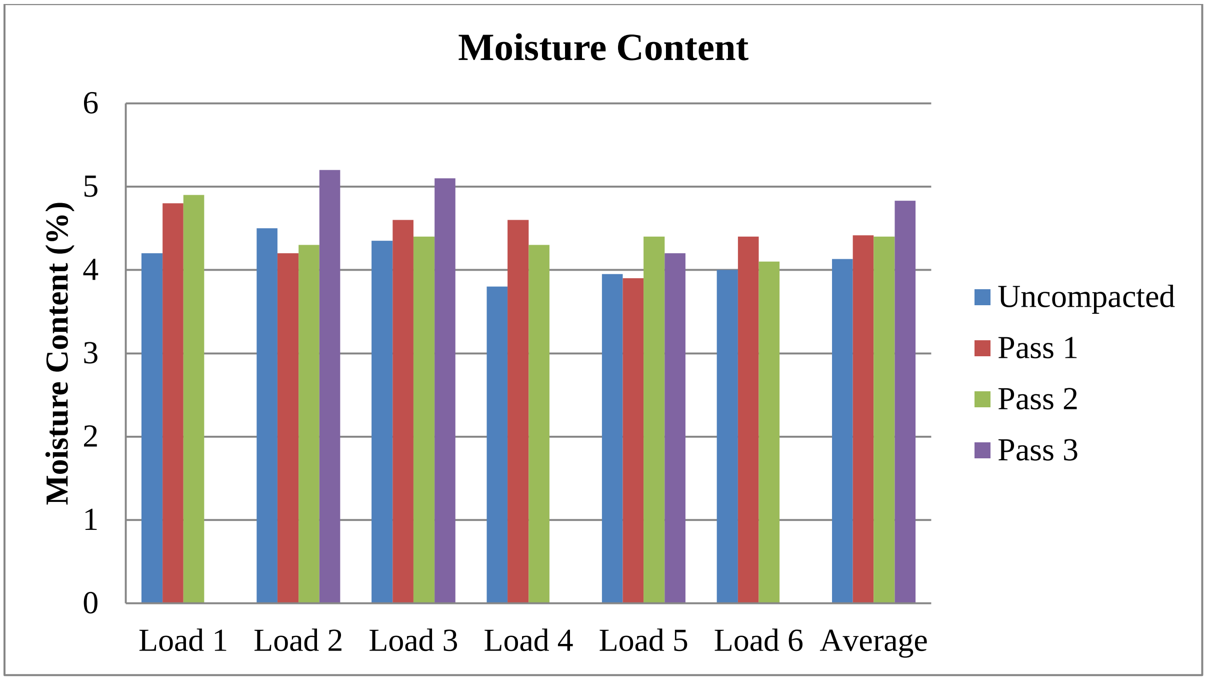

Figure 47: RCC Moisture Results

General Surface Comparison

This purpose of this section is to do a qualitative/general comparison of the surface textures used in cells 5 and 6 to similar to textures on existing cells at MnROAD. The transverse broom in cell 5 will be compared to a longitudinal broom surface in cell 14 (constructed in October 2008). The longitudinal tine in cell 6 will be compared to the ultimate diamond grind in cell 71 (constructed in May 2010). Finally, the transverse boom/conventional grind in cell 5 (the second half of cell 5, 305 and 405, has an existing diamond grind texture) can be compared to the conventional grind in cell 71. Pavement Noise (OBSI), texture (MPD), and friction (FN) results will be used for this comparison.

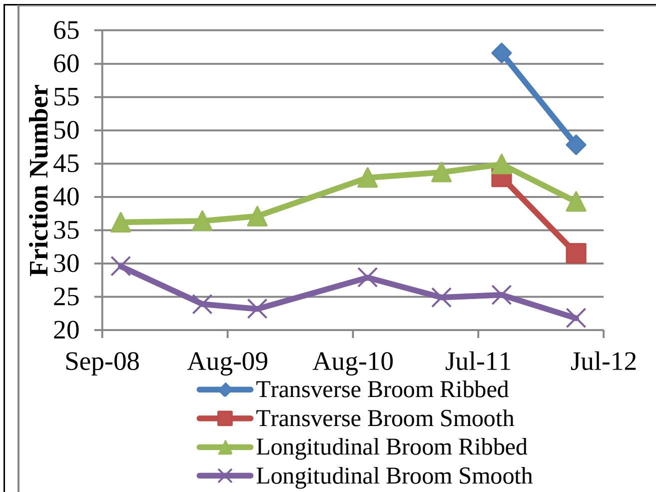

FN, Cells 5 & 14 (Driving Lanes)

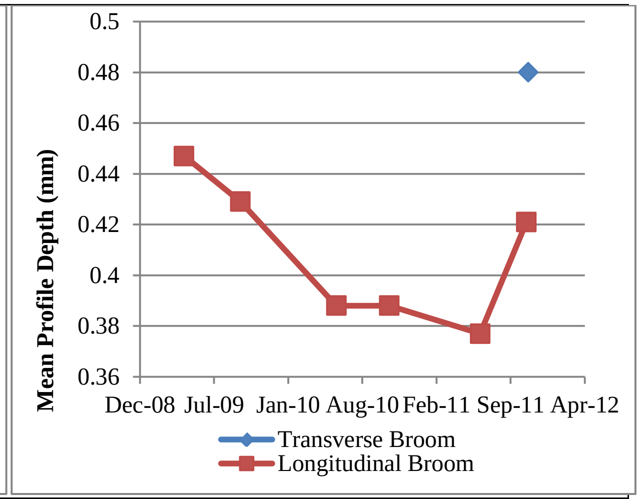

MPD, Cells 5 & 14 (Driving Lanes)

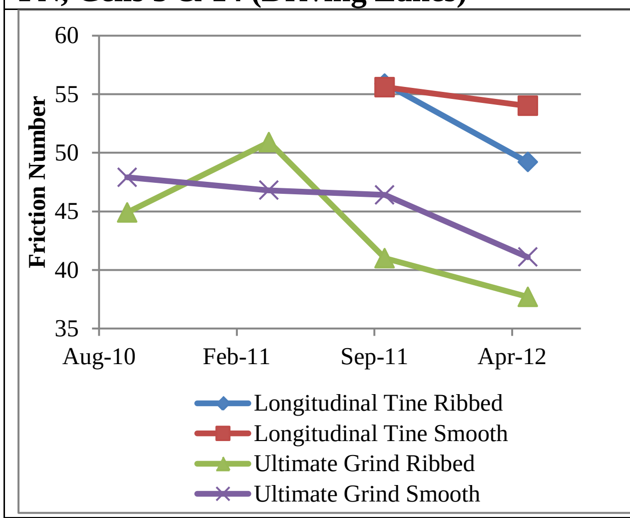

FN, Cells 6 & 71 (Driving Lanes)

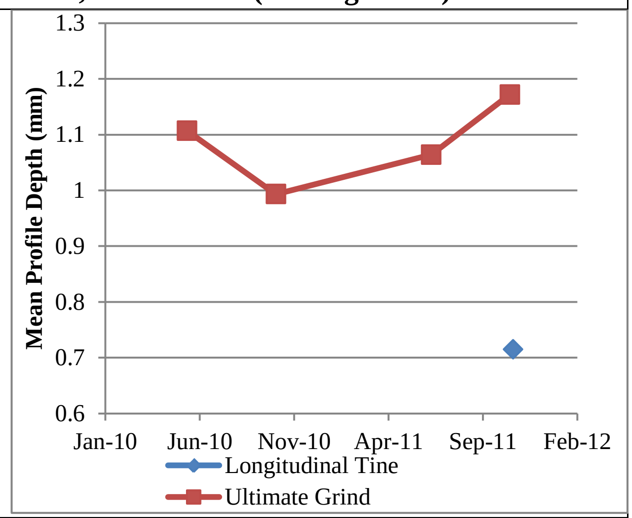

MPD, Cells 6 and 71 (Driving Lanes)

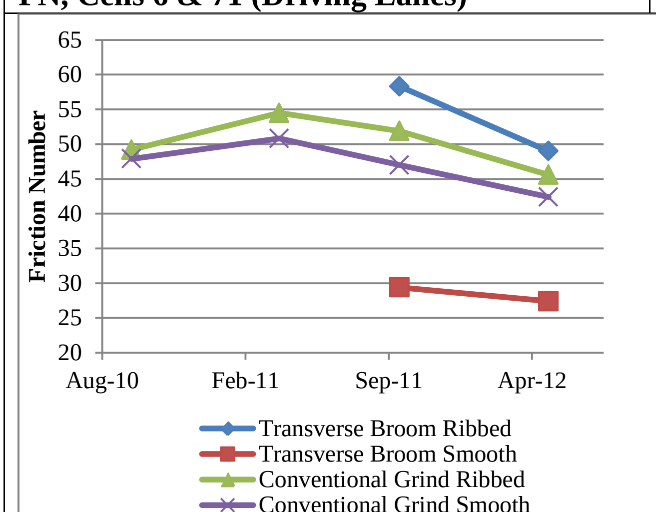

FN, Cells 5 & 71 (Passing Lanes)

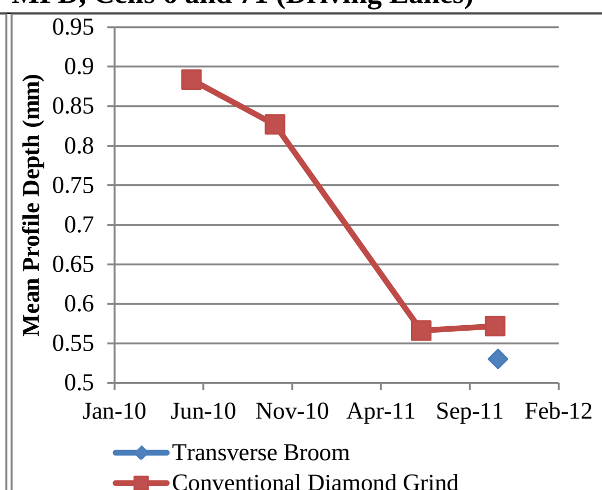

MPD, Cells 5 & 71 (Passing Lanes)

Figure 48: FN and MPD Surface Comparison

The transverse broom has higher friction and MPD than the longitudinal broom. The Longitudinal tine has higher friction than the ultimate diamond grind, however the MPD for the longitudinal tine is lower than the ultimate diamond grind. Friction number trends between the transverse broom and conventional diamond grind are dependent on the type of tire used, however MPD seems to be lower for the transverse broom than the conventional diamond grind.

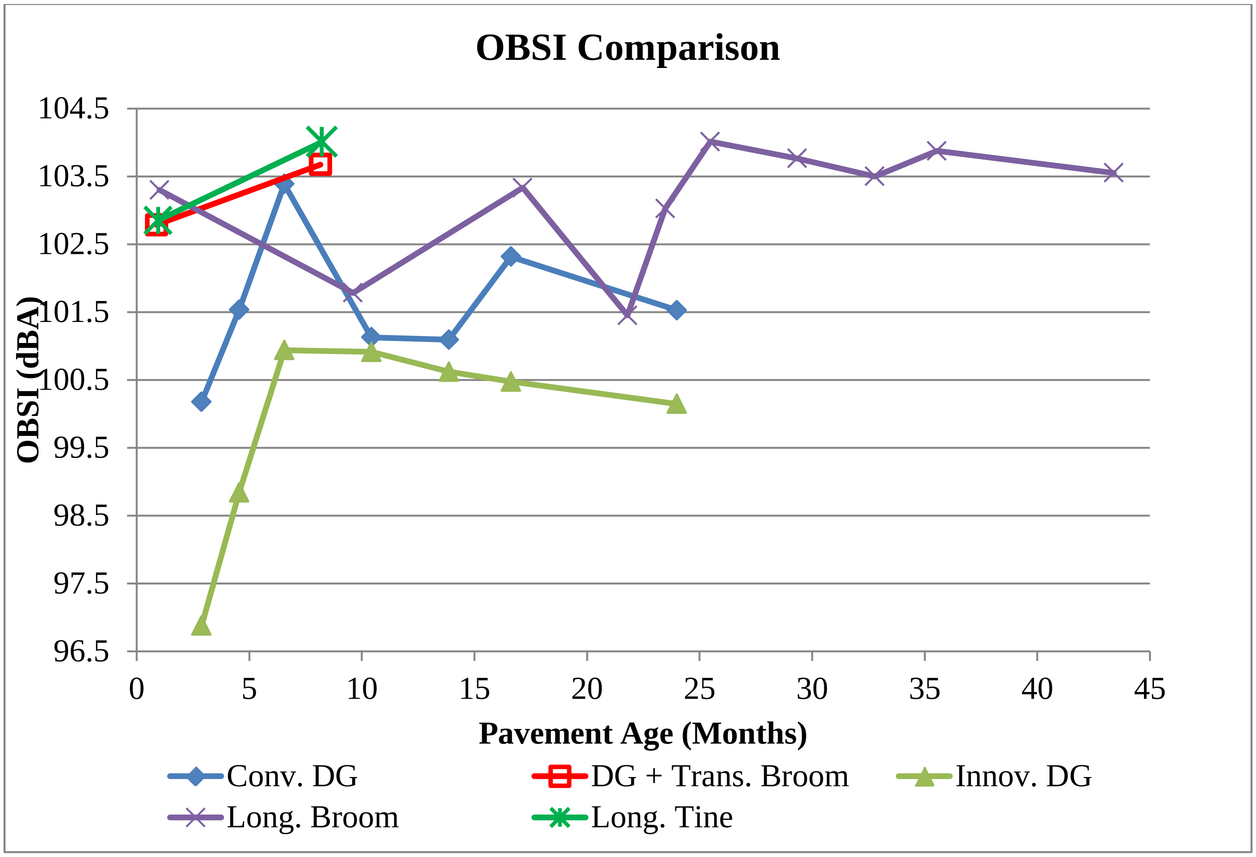

Figure 49: OBSI Surface Comparison

The plot above shows that the longitudinal tine in cell 6 and diamond grind plus transverse broom in in cell 5 is generally trending higher in OBSI than the other surface textures in the comparison with respect to pavement age.

The following plots are shown to provide further comparison between longitudinal tine and diamond grind. The driving lane in cell 71 is the ultimate diamond grind, whereas the passing lane in cell 71 is the traditional diamond grind. The data presented is from the first measurement taken after each cell was constructed.

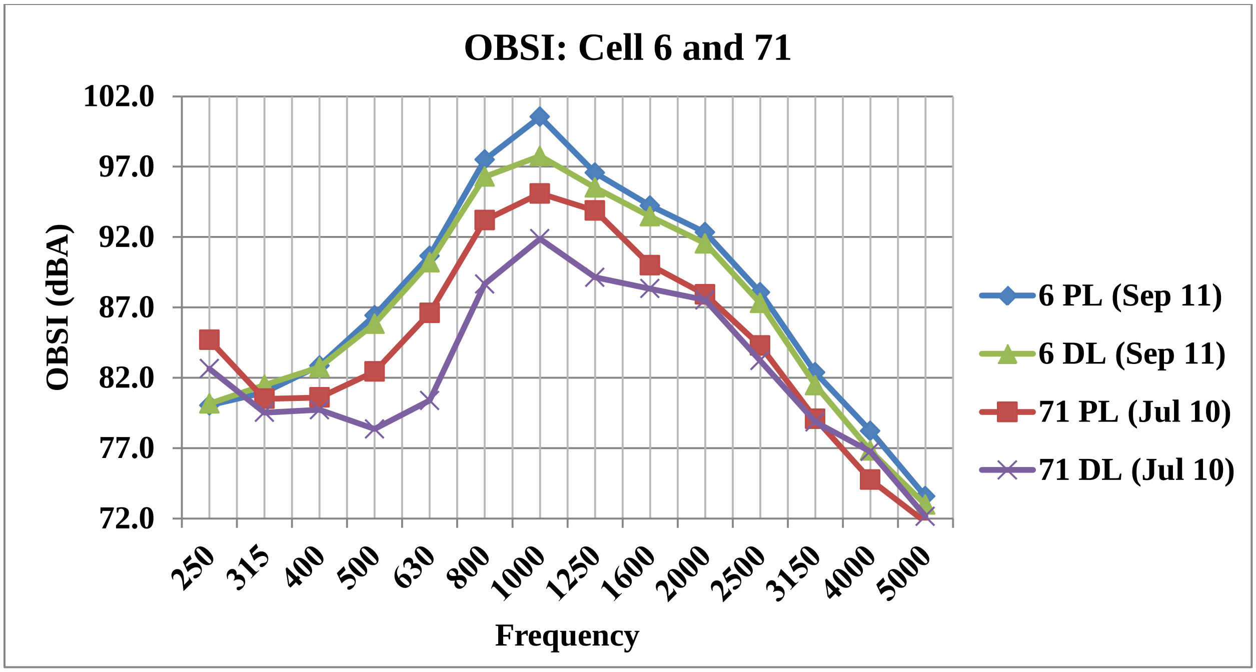

Figure 50: Cell 6 and Cell 71 OBSI Spectrum

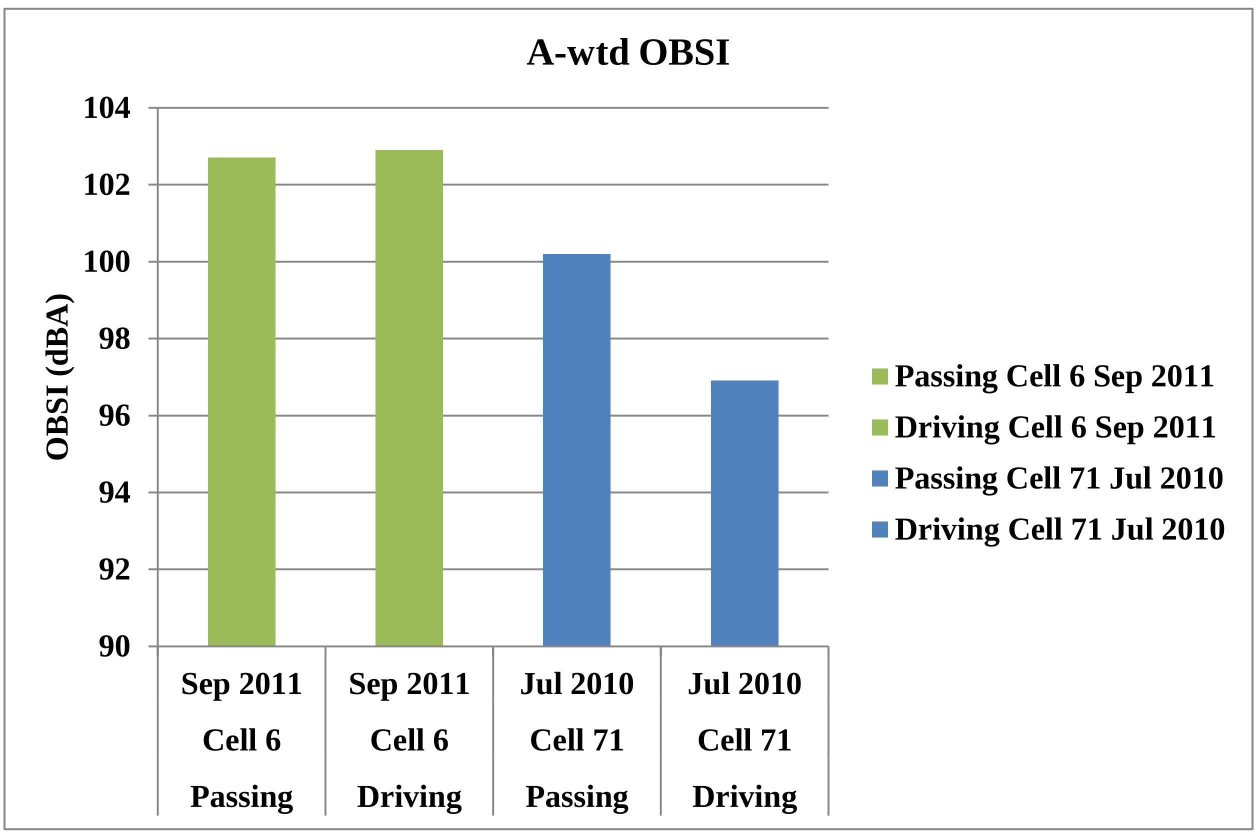

Figure 51: Cell 6 and Cell 71 A-wtd OBSI

From the plots above, you can clearly see that the longitudinal tine has a higher OBSI than both the traditional diamond grind and the ultimate diamond grind.

Cell 63 Rehab

The following plots are provided to evaluate how the repairs done on the thin whitetopping in cell 63 improved performance.

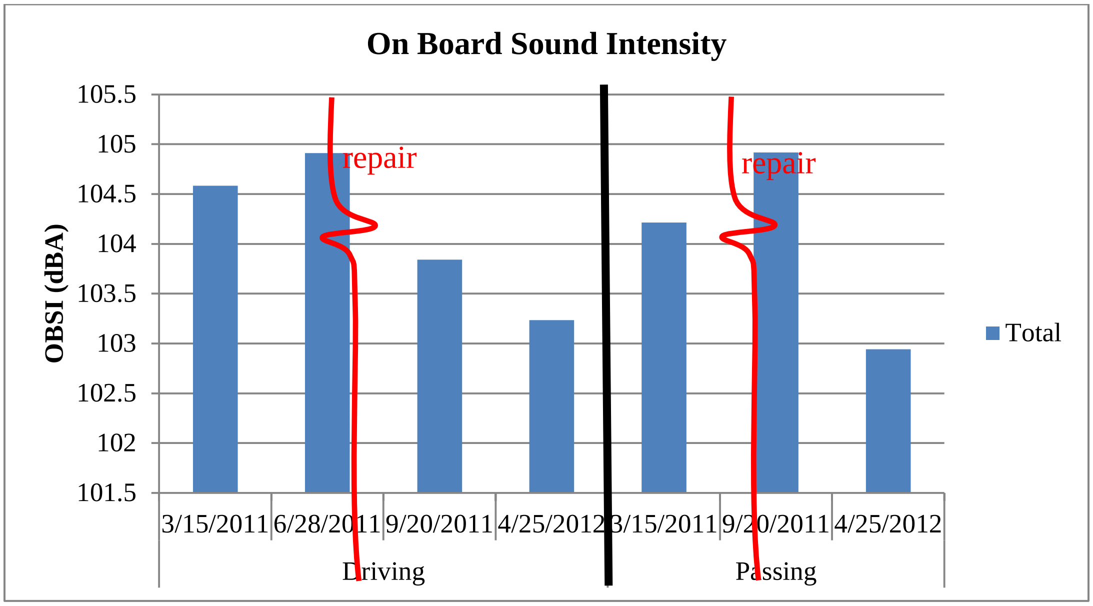

Figure 52: Cell 63 OBSI

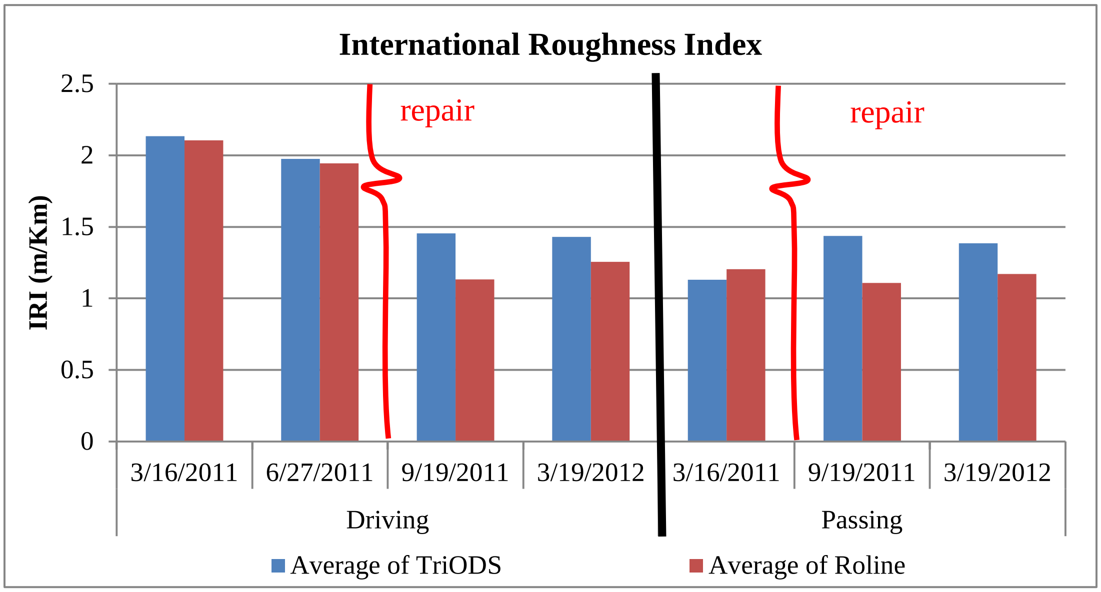

Figure 53: Cell 63 IRI

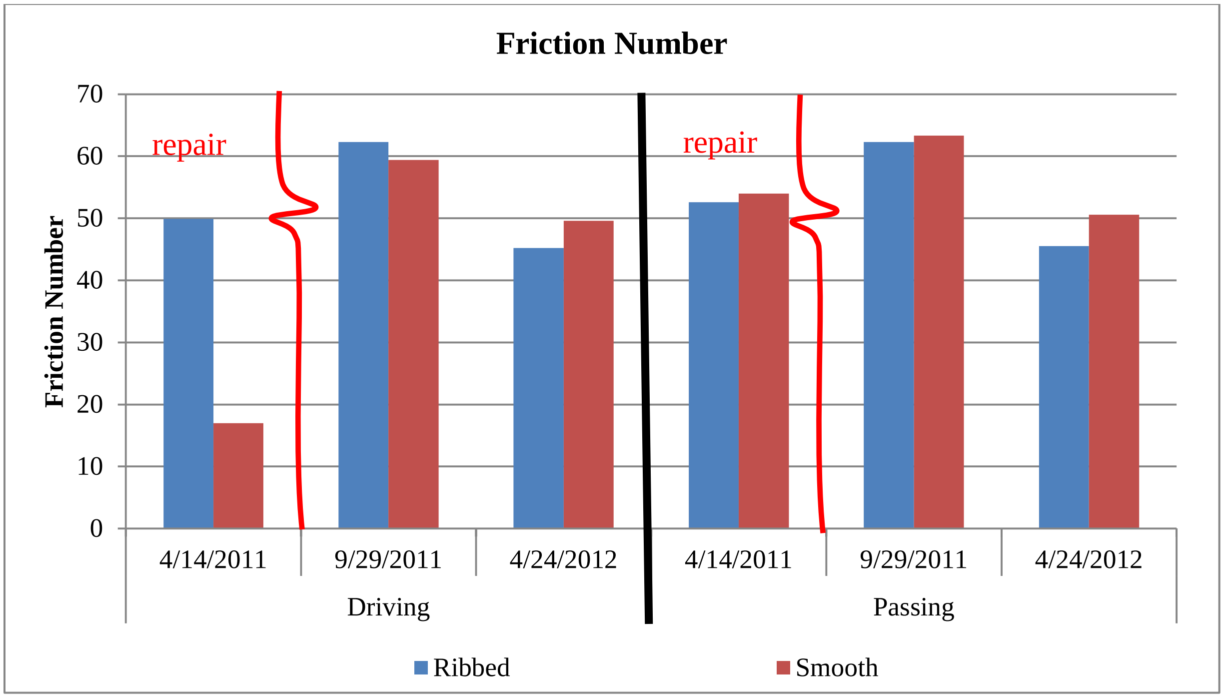

Figure 54: Cell 63 Friction

From these plots, you can see that there are opposite trends in the change in OBSI due to the repairs between the driving lane and passing lane. In the driving lane, repairs showed to decrease the OBSI, whereas in the passing lane, repairs showed to increase OBSI. This trend is also true for ride, where in the driving lane ride is improved after repairs, and in the passing lane, IRI values are slightly increased. The results from friction testing are not as clear. It is possible that the broom finishing done on the repaired panels was flattened during the winter snow removal operations, causing lower friction in the spring. It seems that friction is greatly improved in the driving lane, but results are not as pronounced in the passing lane. Although friction in the passing lane was increase in the fall (for the passing lane), it dropped again in the spring.

Dynamic Load Testing

The performance of an unbonded concrete overlay depends highly on the material used to separate the two layers. In particular, one of the main roles of the interlayer is to prevent reflective cracking in the new pavement from existing distress in the underlying pavement. Below is a theorized stress distribution (Khazanovich) in the bottom of an overlay at the pavement edge for two cases: when the load is applied to an overlay with a noncracked underlying slab, and when the load is applied at a crack (or joint) in the underlying slab. You can see that when the load is applied in a noncracked slab, the increase in stress is gradual. Whereas when the load is applied at a crack in the underlying pavement, the stress drastically increases only near the crack.

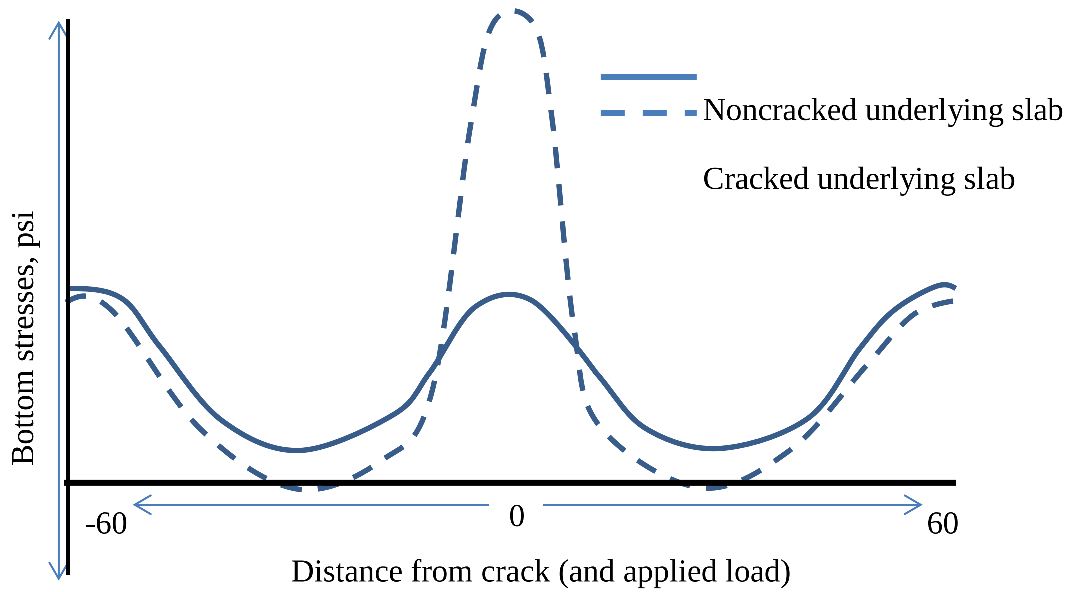

Figure 55: Stress Distribution over Crack

It is hypothesized that stress relief layers, such as the non-woven geotextile used in cell 5, can attenuate this effect of increased stresses at a crack in underlying pavement, which in turn can mitigate issues such as reflective cracking. To investigate the potential of this fabric to provide stress relief at cracks, the strain due to axle loads in the overlay pavement of cell 5 at a joint in the underlying pavement (equivalent to a crack for this purpose) is compared to the strain in the overlay at midpanel of the underlying pavement.

As shown in a previous section of this report, dynamic load response sensors were installed in cell 5 to capture the pavements response to the axle loads from the 80 kip 5 axle tractor-trailer which travels on the low volume road. These sensors were placed in two locations, at a joint in the existing underlaying pavement, and at midpanel of the new overlay pavement (not above an existing joint). This placement is detailed in Figure 56 below. The green blocks represent vertical trees of three sensors at different depths throughout the pavement.The first is placed at the top of the new pavement (0.5 inches) and the second at the bottom of the new pavement (4.5 inches). The third sensor was retrofitted in to the existing pavement before the fabric was laid. These sensors were placed at a depth of 0.5 inches into the existing pavement. The sensors are labeled with numbers in Figure 57 for reference in the plots of measured strain results. The first refers to the sensor in the top of the new pavement and the last refers to the sensor in the underlying pavement. The letter “b” in the label block refers to sensors that have returned zero data after installation.

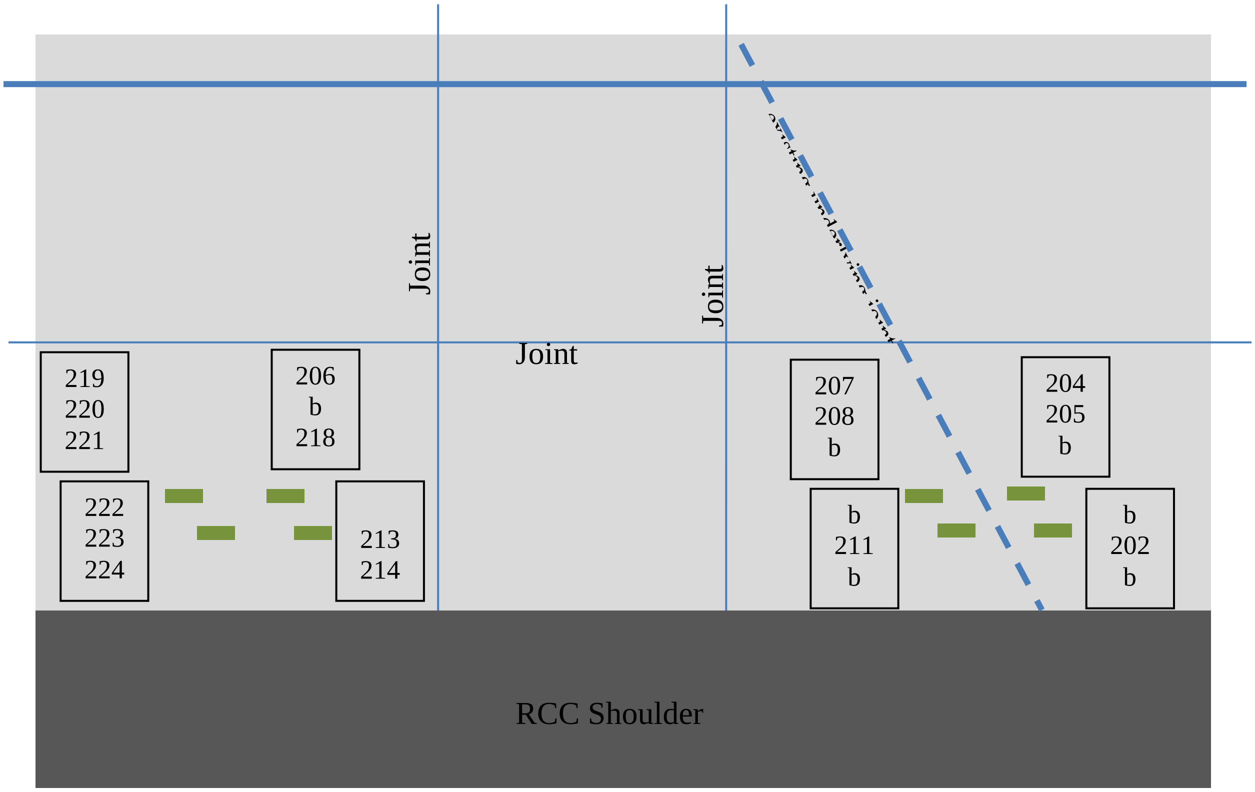

Figure 56: Cell 5 Dynamic Strain Gauge Layout Plan View

For example, sensors labeled 213 to 215 in the box in the picture above are aligned vertically throughout the depth of the new pavement and existing pavement.

The following two figures show cross sections for two sensor trees (aligned in the direction of traffic) at both a joint and at mid panel.

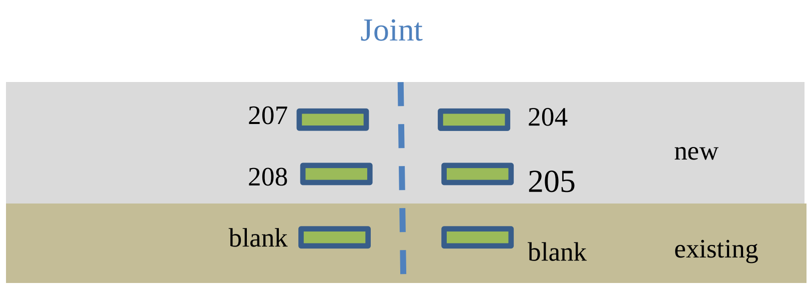

Figure 57: Example of Sensor Layout Cross Section at Joint

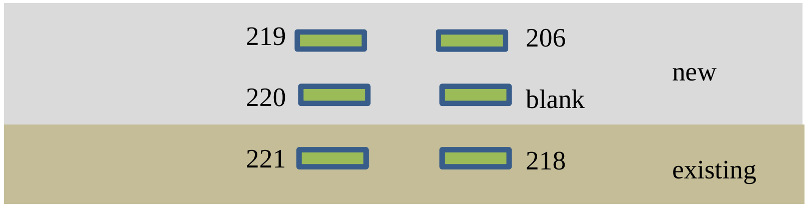

Figure 58: Example of Sensor Layout Cross Section Mid Panel

The sensors are wired to a trigger which initiates data collection as the load from the tractor-trailer approaches. This allows the sensors to capture the response from the load of each of the 5 axles as they pass over the sensor. The sensors return the raw data, requiring a program to analyze the data and determine the baseline strain and peak load responses from each of the five axles.

A “peak-picking” program written in MATLAB software previously developed by MnDOT was used to filter the noise out of the sensor output, and either automatically or manually (selected by the user) determine the baseline strain, axle responses (peak strain from load) and inflection points. The program can also determine intermediate baseline strains when appropriate. The following figure is an example of the raw sensor output (top plot) and the denoised output using the Peak Pick program, highlighting the baseline, inflection points, and axle responses.

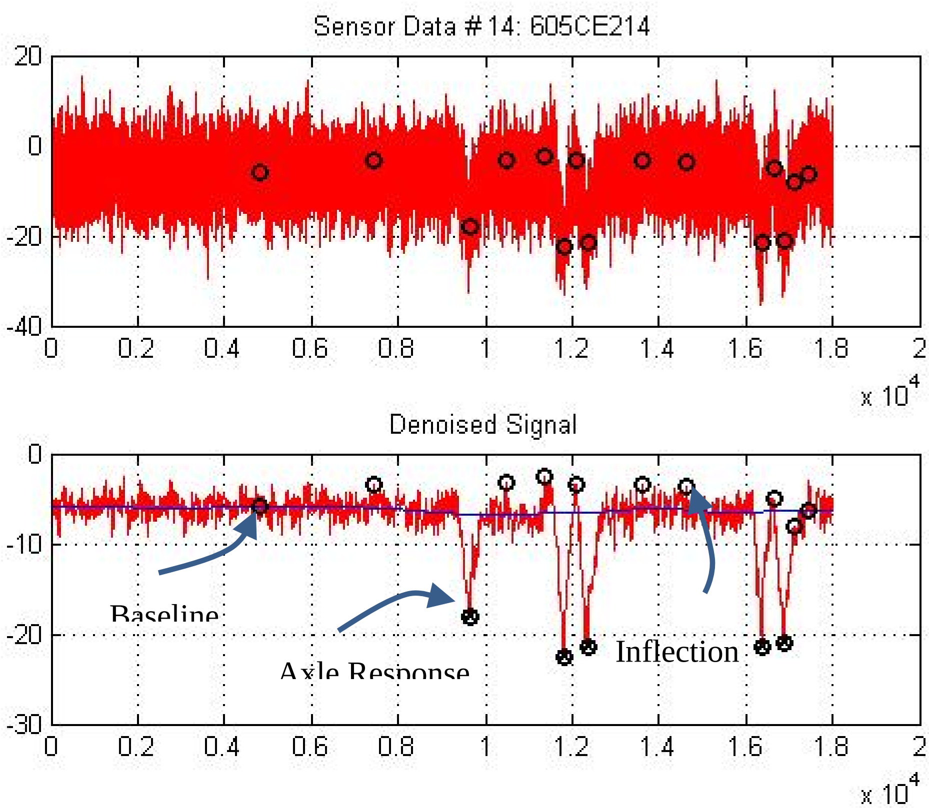

Figure 59: Example of Peak Pick Result

The following plots were made using data collected from dynamic load testing in Fall 2011 (soon after construction) in cell 5 at MnROAD. The values presented are the differences between peak strain and the baseline for each of the five axle responses, and are shown as an averages of all runs at each sensor. Note that “strain – baseline” is intentionally unitless on the plots as these values are only presented for comparison purposes between the sensors at existing joints versus those which are not.

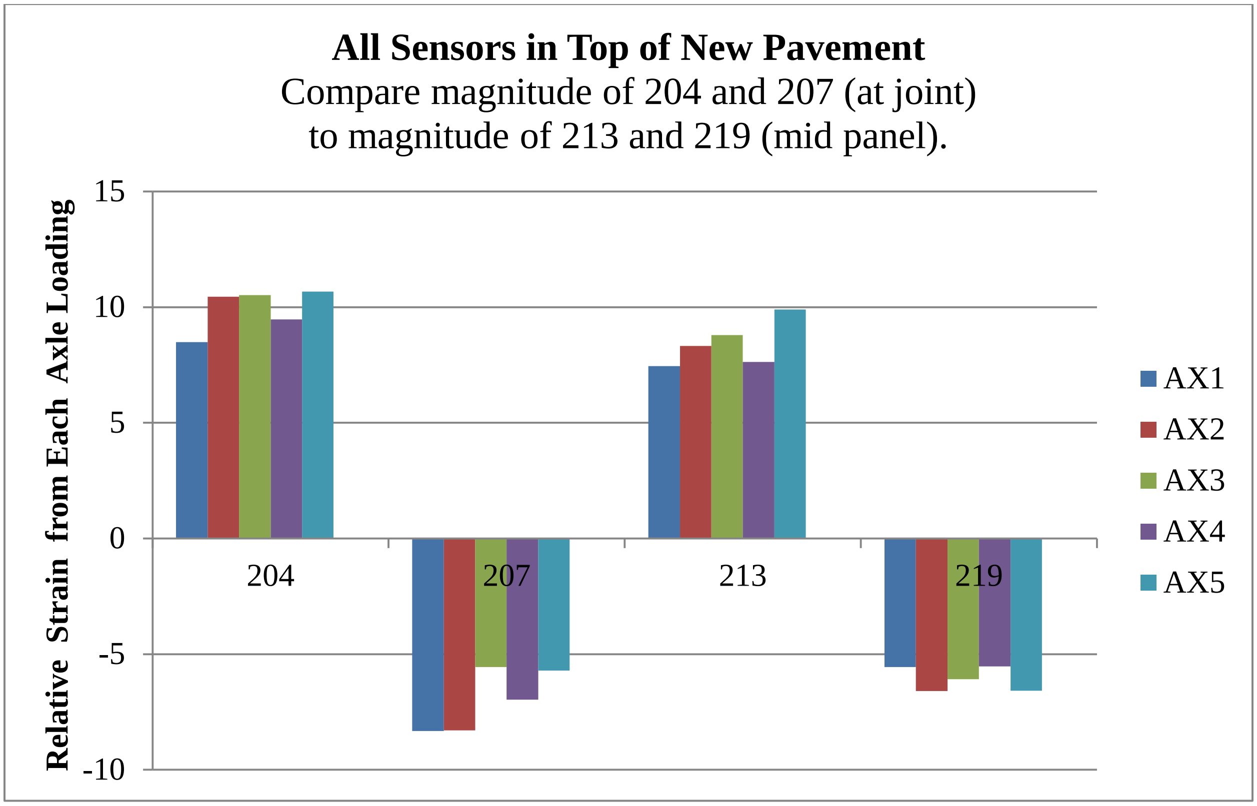

Figure 60: Strain at Top of Pavement from Axle Load

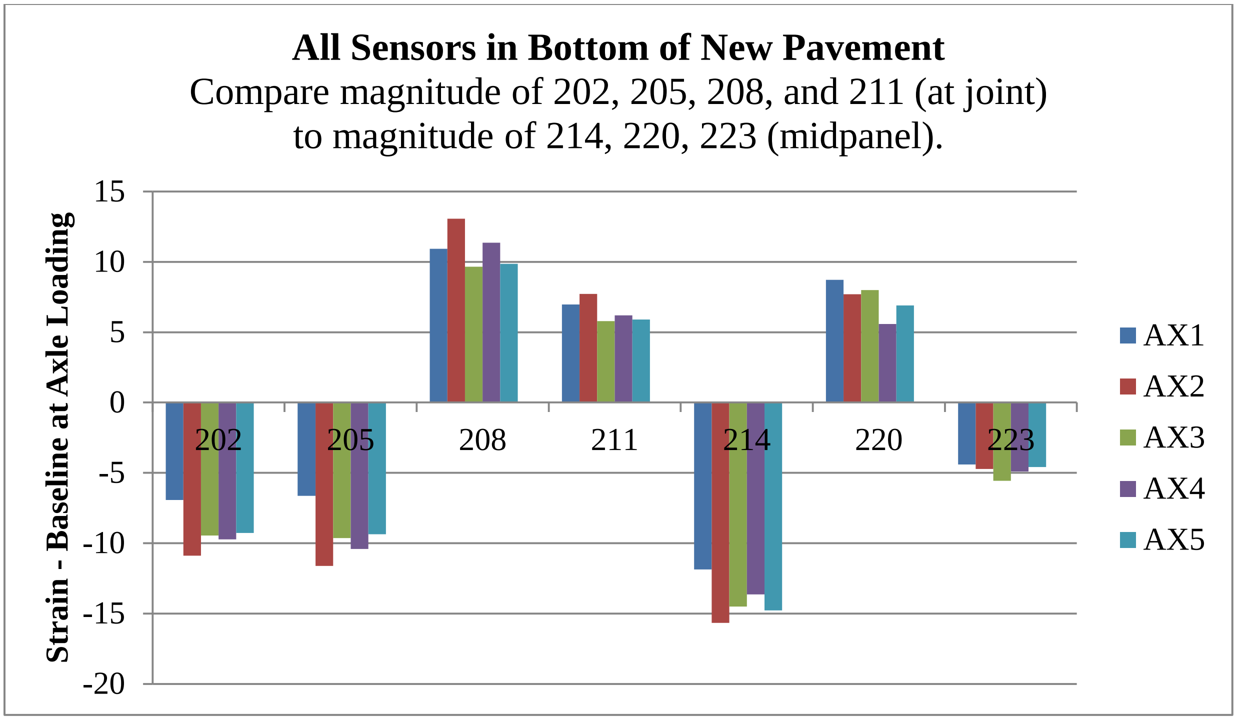

Figure 61: Strain at Mid-Depth from Axle Load

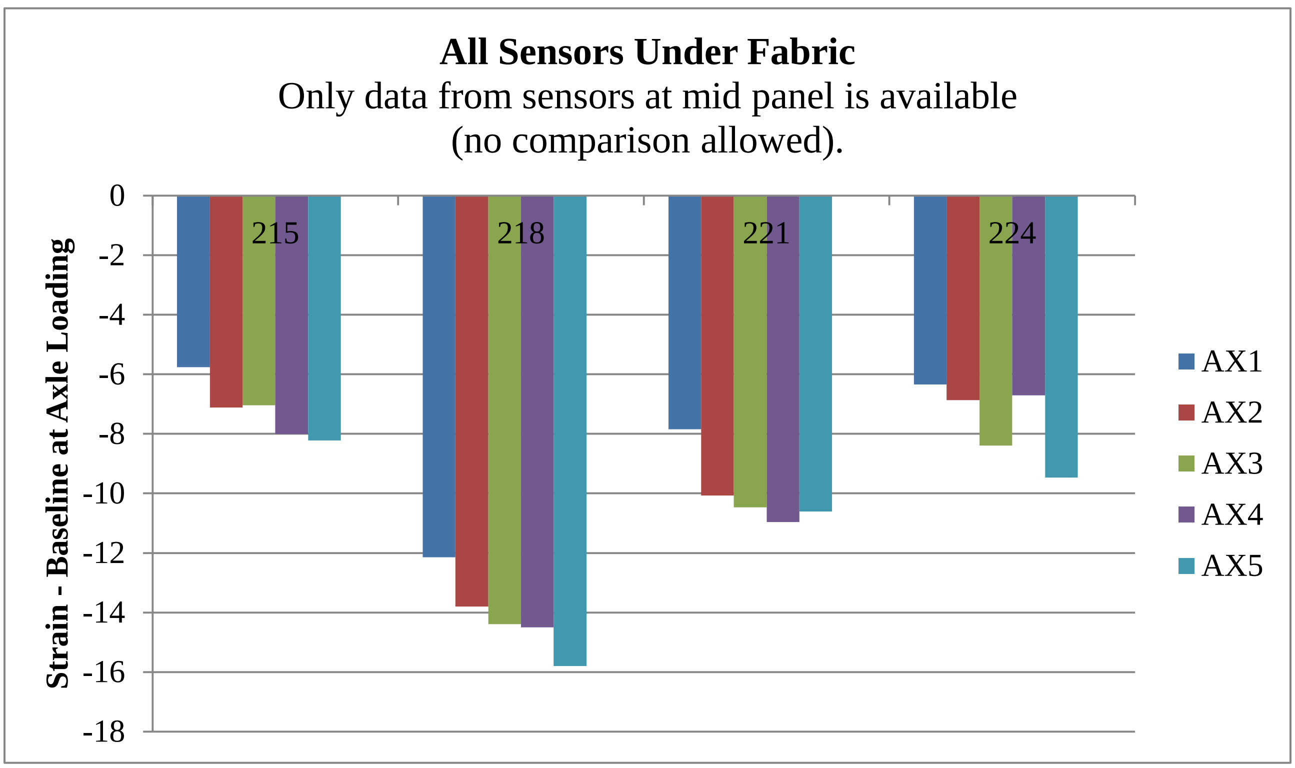

Figure 62: Strain under Fabric from Axle Load

Again, the main purpose of these plots is to compare the magnitude of the response between the two locations. For the purpose of this discussion, the sign (positive or negative) of the strain can be ignored as we are only concerned with the extent of the change in strain during loading. As discussed earlier, it is theorized that the stress relief layer (fabric) in between the existing pavement and new overlay pavement can reduce stresses at existing cracks and joints in the underlying pavement. If the fabric was not contributing to stress relief, we would expect to see much higher magnitude strains at the sensors installed around the existing joint compared to those mid panel. However, the plot show that the magnitudes of these strains at both locations are comparable. Strains at the joint are never drastically higher, and are sometimes lower, than those at the mid panel. This is true for both the sensors at the top of the overlay pavement and those at the bottom of the overlay pavement. Unfortunately, the sensors which were retrofitted in the existing pavement at the joint did not record any data during this testing, but for completeness (and comparison to those in the overly pavement) purposes, the results from sensors in the underlying pavement at mid panel are included.

These results suggest that the geotextile fabric has the potential to provide stress attenuation at cracks and joints in existing substrate pavement. However, these results and very basic analysis are only considered preliminary. Further research, data collection, and more complex analysis will be required to ascertain if this hypothesis is true.

CHAPTER 7: CONCLUSION

The following conclusions are based on an early performance evaluation of reconstruction of two full-depth concrete pavement test sections, including RCC shoulders on both sections, along with repair of a thin whitetopping test cell at MnROAD.

- Based on limited extensive laboratory and field observations, the gradation used to achieve the drainable base in one test section at MnROAD appears to provide stability and permeability.
- Transverse broom appears to provide more friction than longitudinal drag. However, the acoustic implication was not very distinct and will require further monitoring.
- Roller compacted technology appeared to be a feasible construction practice. However, this initiative requires much care in mix design, including an elaborate process of trial mixing and density testing, to arrive at a useable mix design. Moreover, the striations arising from roller compaction appear to be little fissures that could, in the long term, facilitate ingress of deicing salts and consequently, early damage to the pavement. This needs further study.
- The surface configuration of RCC likely needs additional texturing for friction enhancement.
- Results from performance testing of cell 63 suggest that rehab may have been successful in reducing pavement noise, providing higher friction, and somewhat improving ride.
- Fabric interlay should provide some stress relief based on the strain distribution with respect to distance from the joint. However, at this stage of monitoring and data analysis, a strong conclusion may be premature.
- Initial results show that a longitudinal tined surface had higher OBSI, higher friction, and a lower mean profile depth when compared to a longitudinal diamond grind. Initial results from a transverse broom surface show higher friction, mean profile depth, and OBSI than a similar pavement finished with a transverse broom surface.

REFERENCES

AASHTO (2009) Stan*dard Method of Test for Measurement of Tire/Pavement Noise Using the On-Board Sound Intensity (OBSI) Method*. AASHTO TP 76-09. American Association of State and Highway Transportation Officials. Washington, D.C.

ASTM (2007) *Standard Test Method for Measuring Deflections with a Light Weight Deflectometer*, ASTM E 2583-07, American Society for Testing and Materials, West Conshohocken, PA.

ASTM (2005) *Standard Test Method for Use of the Dynamic Cone Penetrometer in Shallow Pavement Applications*, ASTM D 6951-03, American Society for Testing and Materials, West Conshohocken, PA.

ASTM (2008) *Standard Practice for Molding Roller-Compacted Concrete in Cylinder Molds Using a Vibrating Hammer*. ASTM C1435-08. American Society for Testing and Materials, West Conshohocken, PA.

ASTM (2012) *Standard Test Method for Compressive Strength of Cylindrical Concrete Specimens*. ASTM C39/C39M-12. American Society for Testing and Materials, West Conshohocken, PA.

ASTM (2010) *Standard Test Method for Flexural Strength of Concrete (Using Simple Beam with Third-Point Loading*. ASTM C78/C78M-10. American Society for Testing and Materials, West Conshohocken, PA.

ASTM (2011) *Standard Test Method for Skid Resistance of Paved Surfaces Using a Full-Scale Tire*. ASTM E274/E274M-11. American Society for Testing and Materials, West Conshohocken, PA.

ASTM (2008) *Standard Specification for Standard Rib Tire for Pavement Skid-Resistance Tests*. ASTM E501-08. American Society for Testing and Materials, West Conshohocken, PA.

ASTM (2008) *Standard Specification for Standard Smooth Tire for Pavement Skid-Resistance Tests*. ASTM E524-08. American Society for Testing and Materials, West Conshohocken, PA.

ASTM (2009) *Standard Test Method for Measuring Pavement Macrotexture Properties Using the Circular Track Meter*. ASTM E2157-09. American Society for Testing and Materials, West Conshohocken, PA.

Davich, P., F. Camargo, B. Larsen, R. Roberson, and J. Siekmeier (2006) *Validation of DCP and LWD Moisture Specifications for Granular Materials*, Report No. 2006-20, Minnesota Department of Transportation, Saint Paul, MN.

Fleming, P.R., M.W. Frost, and J.P. Lambert (2007) "Review of Lightweight Deflectometer for Routine In Situ Assessment of Pavement Material Stiffness," *Transportation Research Record*. No. 2004. pp 80-87.

Khazanovich, Lev. *Improved Concrete Overlay Design Parameters for Airfield Pavements*. ERES Consultants. IPRF Research Report DOT/FAA-01-G-002-2. Washington, D.C.

Mooney, M.A. and P.K. Miller (2009) "Analysis of Light Weight Deflectometer Test Based on In Situ Stress and Strain Response," *Journal of Geotechnical and Geoenvironmental Engineering*, Vol. 135, No. 2. pp 199-208.

Mooney, M.A., C.S. Nocks, K.L. Selden, G.T. Bee, and C.T. Senseney (2009) *Improving Quality Assurance of MSE Wall and Bridge Approach Earthwork Compaction*, Report No. CDOT-2008-11, Colorado Department of Transportation, Denver, CO.

Newcomb, D.E. and B. Birgisson (1999) *Measuring In Situ Mechanical Properties of Pavement Subgrade Soils*, NCHRP Synthesis of Highway Practice Report 278, National Academy Press, Washington D.C.

Oman, M. (2004) *Advancement of Grading & Base Material Testing*, Office of Materials, Minnesota Department of Transportation, Maplewood, MN.

Vennapusa, P and D. White (2009) "Comparison of Light Weight Deflectometer Measurements for Pavement Foundation Materials," *Geotechnical Testing Journal*. Volume 32, Issue 3. pp 1-13.

White, D., M. Thompson, and P. Vennapusa (2007) *Field Validation of Intelligent Compaction Monitoring Technology for Unbound Materials*, Report No. 2007-10, Minnesota Department of Transportation, Saint Paul, MN.

APPENDIX A: MNROAD TEST SECTION LAYOUTS

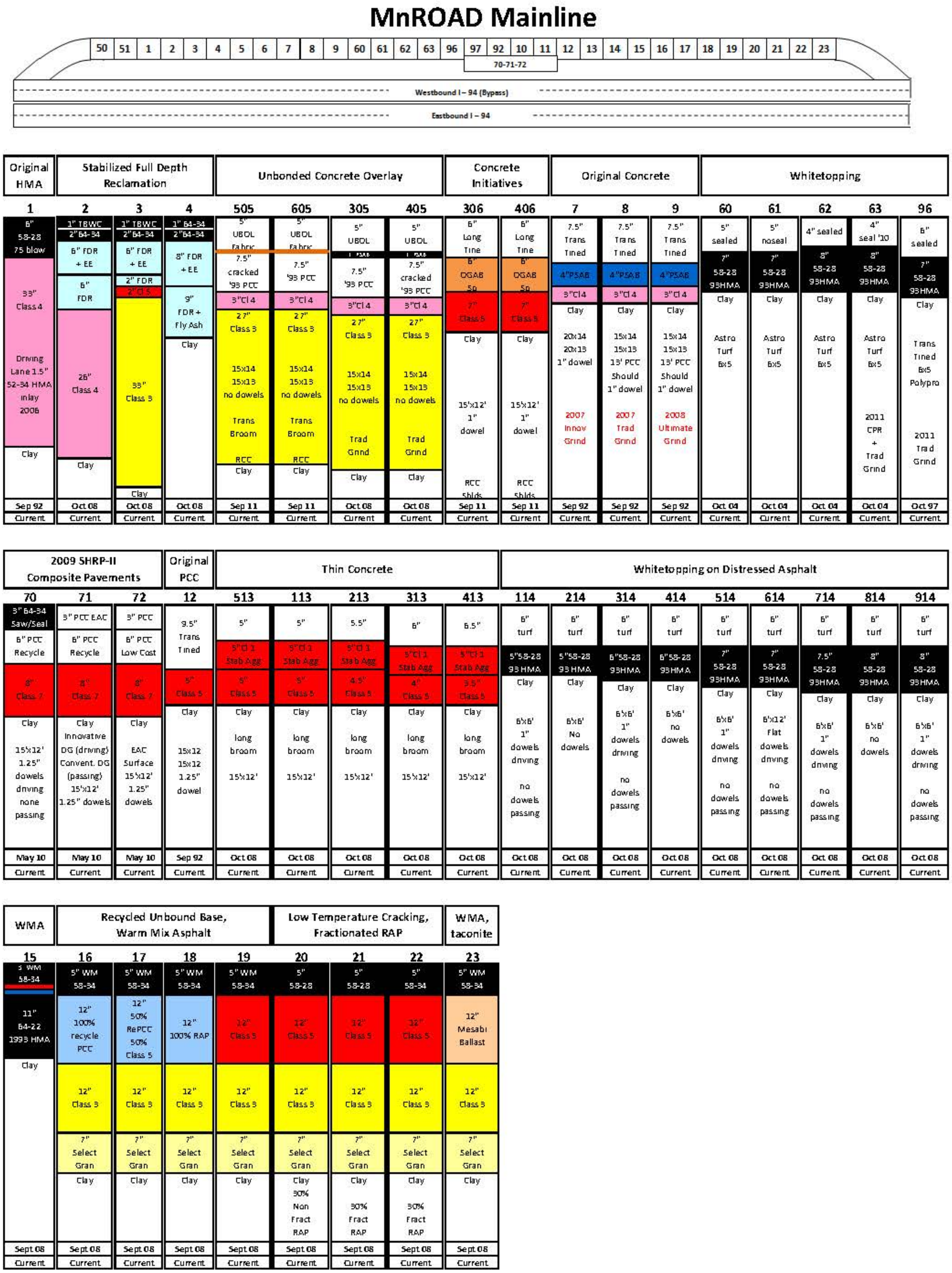

* All thicknesses shown as design thickness

Figure A-1. MnROAD Test Cell Layout (Mainline)

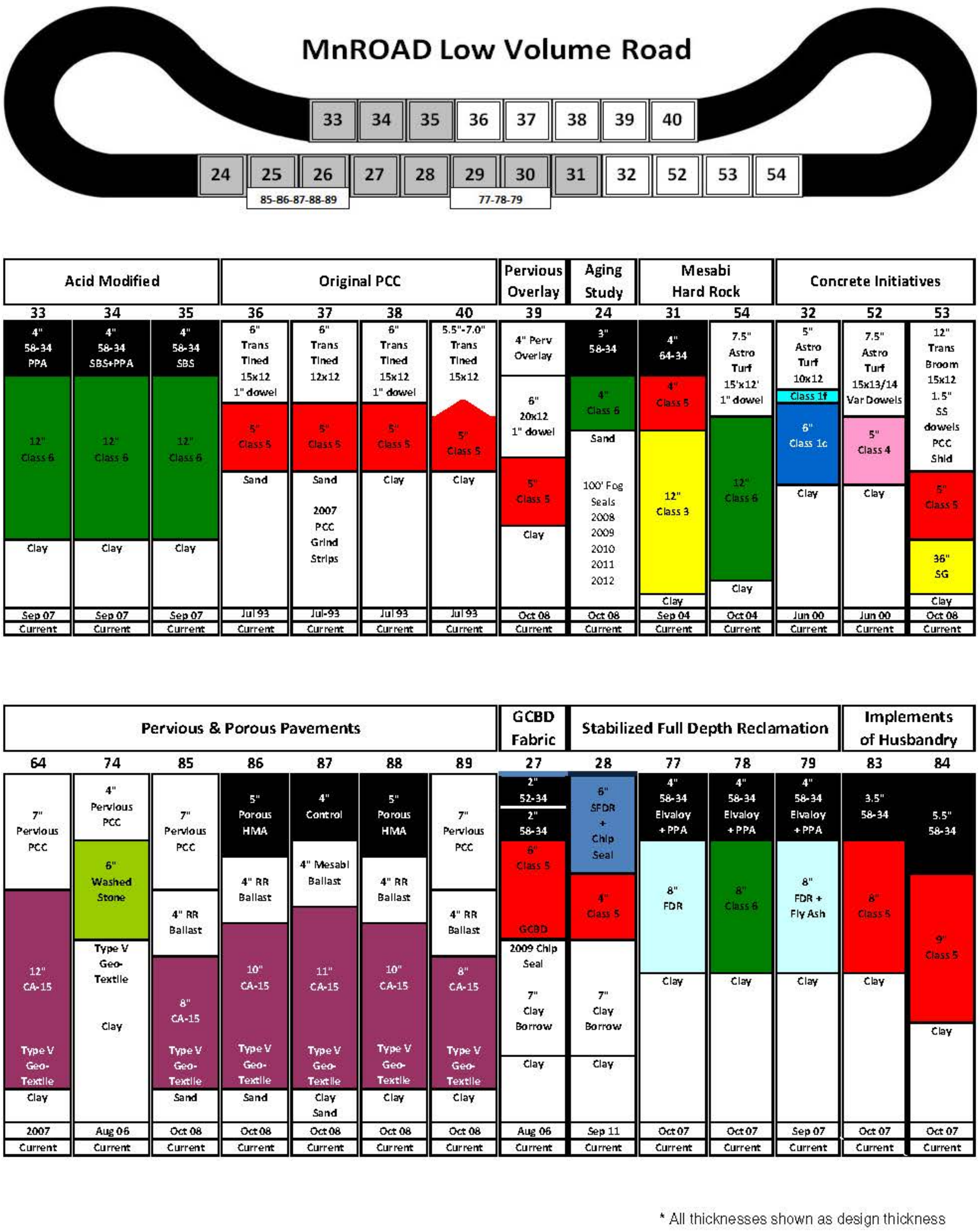

Figure A-2. MnROAD Test Cell Layout (Low Volume Road)

APPENDIX B: PERMEABILITY TEST REPORT

Constant Head Permeability Test

Minnesota Department of Transportation
Foundations Unit

Date of Test: November 28, 2011
Date of Report: December 20, 2011

Introduction

The ability of a soil to transmit water is defined as the soils permeability. For road building applications, it is often necessary for an engineer to estimate the permeability of a soil to ensure proper drainage. In soil mechanics, this property can be expressed as a velocity known as the Coefficient of Permeability, ***k***. A soil with a small value for ***k*** indicates more resistance to flow. Conversely, if the value of ***k*** is higher, the soil has a greater capacity for water flow. The Constant Head Permeability Test is used to determine the ***k*** value of sands and gravels. For measuring permeability in cohesive soils the Falling Head Permeability Test should be used (but will not be discussed in this report).

Theory

In saturated conditions, one-dimensional flow is governed by Darcy's Law (Eq. 1). Essentially, this law states that flow velocity is proportional to the hydraulic gradient.

Eq. 1

$$v = ki$$

Where:

	v	= flow velocity = Q/At
	Q	= quantity of water discharged
	A	= area in which water flow occurs (area of test apparatus)
	t	= total time of water discharge
	k	= coefficient of permeability
	i	= the hydraulic gradient = (h/ L)
	h	= difference in head between two points
	L	= Length between two points

Solving for ***k***, we arrive at:

Eq. 2

$$k = \frac{QL}{Ath}$$

All values from the above equations, which the exception of ***k***, can be directly measured from the test.

Procedure

The procedure for this test closely followed ASTM D 2434-68 Standard Test Method for Permeability of Granular Soils (Constant Head). The compaction method chosen for the soil was Compaction by Sliding Weight Tamper. Additionally, two methods were used to develop the increasing flow through the test apparatus. First, the flow was increased by slightly adjusting the outflow valve for seven tests (see Figure 1), until the valve was fully open. Next, we ran six additional tests in which the flow was increased by raising the hydraulic head in the system. This was achieved by increasing the elevation of the constant head basin for each test point while the outflow valve was fully open (see Figure 2). In the ASTM, it is prescribed that the basin elevation be raised in 0.5 inch increments; however our set up only allows increasing the basin elevation in 1.0 inch increments.

It should also be noted that the two pressures in the tests were not measured by manometers as described in the ASTM, but instead by pressure transducers that were read via computer. This system allows a high degree of accuracy and tracking of pressure changes within the sample allowing an easier determination of steady-state conditions.

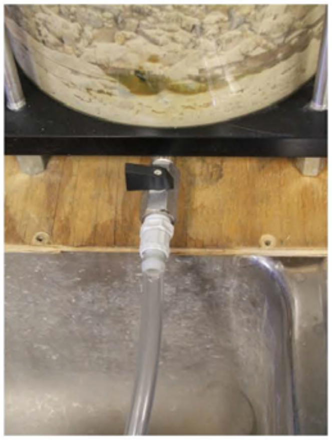

Figure 1 – Outflow Control Valve

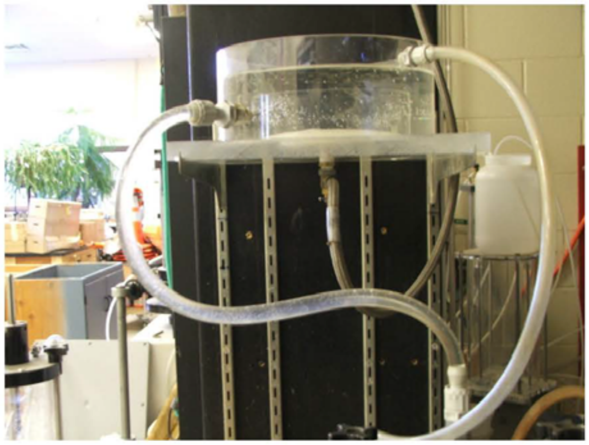

Figure 2 – Constant-Head Basin

Experiment Results

The test was run 13 times, seven of the tests were run by adjusting the outflow valve, and six increased the hydraulic head (the height of the water basin). The average value for the coefficient of permeability (K_{avg}) for these 13 tests was 0.0068 cm/sec. (see attached chart) with the average water temperature throughout the tests of 17.6 °C.

Discussion

During the test, the finer soil particles were seen washing to the bottom of the apparatus (See Figure 3). It was postulated that because the sample was not well graded, there were easy flow paths, through gaps between larger particles, for the fine grains to travel with the water flow. It was noticed during the initial tests that grains were cascading down as the water was allowed to flow through the apparatus. Interestingly, this material was shown to shed finer-grained materials in the field as well.

As a result, the coefficient of permeability that was determined from this test is lower than what would be expected from the sample. The new K_{avg} = 0.0068 cm/sec. This puts the value under the typical range for fine sand. Typical ranges for permeability are as follows:

Clean Gravel	100 to 1 cm/sec
Coarse Sand	1 to 0.01 cm/sec
Fine Sand	0.01 to 0.001 cm/sec
Silt	0.001 to 0.00001 cm/sec

Clay <0.000001 cm/sec

It could be argued that this does not represent how the sample would perform in the field. In the real world, it is possible that the fines (if washed out of a layer of this material) would not control the permeability. The fines in this test covered the only possible flow path for the water, which is out the bottom valve. In the field, the water might find other paths that are less likely to get clogged with the finer material, such as out the sides of the embankment.

Figure 3 - Test apparatus after the tests were run.

It is known that the Constant Head Permeability test can produce highly variable results even on samples taken from the same source. One test to another can vary as much as an order of magnitude or more. The reasons for this variability change test to test, but generally are confined to six soil properties:

1) Porosity
2) Particle-size distribution
3) Shape and orientation of soil particles
4) Degree of saturation/presence of air
5) Type of cation and thickness of adsorbed layers associated with clay minerals (if present)
6) Viscosity of the soil water

It is likely that the permeability of this sample is controlled by the first three in the list. By simply re-running the test with another sample, these three parameters can be changed enough to result in a very different permeability.

Conclusion

Since the value for ***k*** was lower than what was expected from the soil, there is a certain amount of uncertainty in the result. However, the test has shown to historically be variable from test to test, and increasing ***k*** by one order of magnitude to 0.068 would put the result in a category which is more expected from this type of sample. Therefore, the result is valid, however additional tests should be run on similar samples in order to verify the results and improve on test procedures.

Attachments: Lab Notes
Test Results Chart

Permeability Test

Water added = (2935.1 + 780) = 3715.1 g
I.D. = 9 in
H = 13 1/8 in

Empty = 8319 g
Sample + Apparatus = 80.55 lbs
Empty Folgers = 163.4

<u>Constant Head, Valve Changing</u>

Test No.	H_1 (mm)	H_2 (mm)	Time (s)	Temp (^oC)	Water (g)	Notes
1	-0.694	-2.7694	300	20.0	730.9	Valve @ 20^o
2	-3.123	-6.2311	300	19.2	1162.3	Valve @ 25^o
3	-3.47	-6.0581	300	18.7	1259.3	Valve @ 33^o
4	-2.776	-4.8464	300	18.3	1223.1	Valve @ 50^o
5	0.1735	-3.1156	300	17.0	1099.7	Valve @ 60^o
6	-3.47	-3.8079	300	16.8	1098.7	Valve @ 75^o
7	-3.47	-3.981	300	16.8	1070.2	Valve @ 90^o (fully open)

Flow rate decreased @ Test 4 + beyond. Fines clogging the valve?

Moisture Sample

Tare = 85.5g
Wet = 780.9g
Dry = 730.9g

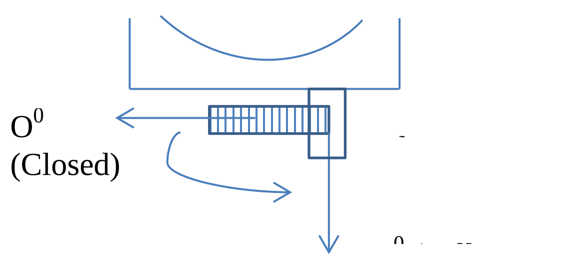

Increasing Head, Gate fully open

Test No.	H_1 (mm)	H_2 (mm)	Time (s)	Temp (^oC)	Water (g)	Notes
7	-0.347	-3.981	300	16.8	1070.2	-6 in (Bottom)
8	26.546	20.77	300	17.1	916.0	-5 in
9	51.877	45.695	300	17.0	919.3	-4 in
10	76.34	69.062	300	17.0	926.5	-3 in
11	104.1	96.236	300	16.8	925.8	-2 in
12	130.82	126.01	300	17.0	927.1	-1 in
13	151.64	146.78	300	16.8	921.4	0 (Top)

ΔH Between H_2O @ 0 and V ≈ 19 in

Height diagram

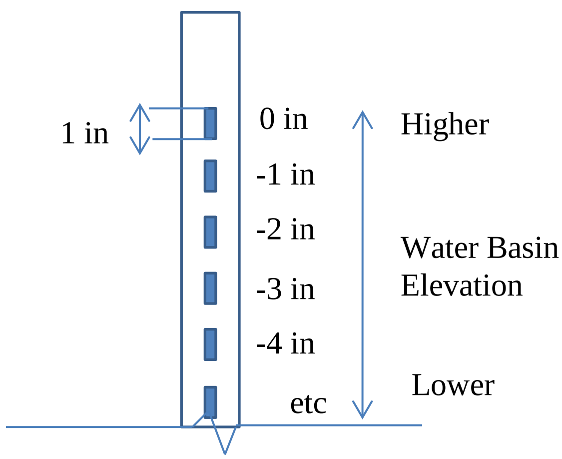

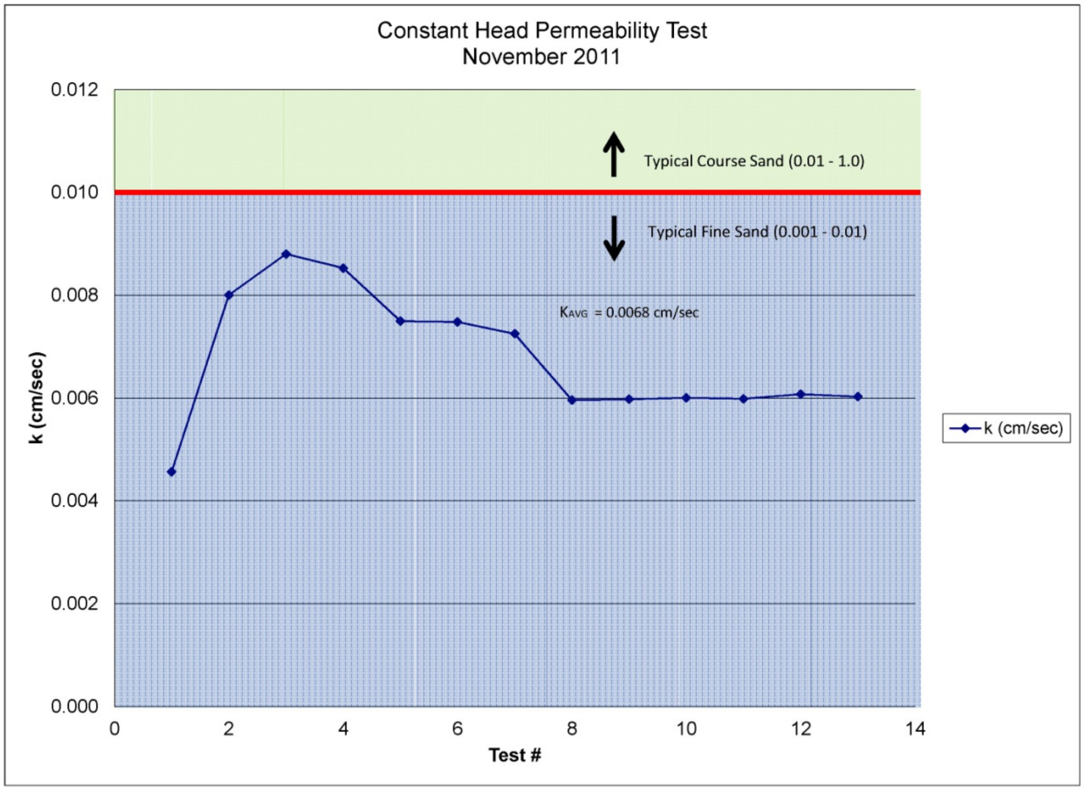
Constant Head Permeability Test
November 2011
Typical Course Sand (0.01 - 1.0)
Typical Fine Sand (0.001 - 0.01)
KAVG = 0.0068 cm/sec
k (cm/sec)
0.012
0.010
0.008
0.006
0.004
0.002
0.000
0
2
4
6
8
10
12
14
Test #
k (cm/sec)

APPENDIX C: TRANSVERSE BROOM PICTURES

APPENDIX D: C.S. MCCROSSON PAVING DIVING CASE STUDY: CONVENTIONAL VS. COMPOSITE PAVING

Conventional vs. Composite Paving

CASE STUDY

By C.S. McCrossan Paving Division

OVERVIEW: To compare the costs of Conventional Concrete Paving with the costs of Composite Paving. Composite Paving or Wet on Wet paving is a process that involves paving the roadway in two lifts. The first lift being one thick, low quality layer of concrete utilizing recycled concrete as the main aggregate with lower percentages of quality aggregates in the mix design. The second lift is a fairly thin high quality layer (2-3 inches) that has high quality aggregates, with none of the recycled material present.

The benefit of Composite Paving is said to be in areas where high quality aggregates are of a high cost or a low supply, and low quality materials throughout one layer is not an option. Composite paving allows the lower layer to be produced using cheaper recycled material, allowing the higher priced or more scarce high quality aggregates to be used in the upper layer. The recycled material in the base layer is not expected to affect the structural quality of the slab as a whole. This makes Composite Paving an attractive option when paving in areas where high quality aggregates are difficult or expensive to find.

OBJECTIVE: Find a project in Minnesota that is located in an area not readily accessible to high quality aggregates. Take the original conventional pavement bid, and compare it to the expected costs of paving had it been bid using Composite Paving techniques. The extra cost of operating two paving operations as well as two batch plants will be compared to the expected costs for the aggregates using recycled material instead of Class A material for the base layer. The objective being to find what the saving on the recycled material would have to be to break even in comparison to the Conventional Method.

PROJECT: U.S. Highway 14 Concrete Paving

LOCATION: Near Waseca, MN

GENERAL STATS:

- 90,000 Cubic Yards of Concrete
    - 80,000 CY Mainline Paving. 310,000 Sq. Yards
    - 10,000 CY Crossroads and Ramps
- 19.5 Miles of paving
- 22 total days mainline paving scheduled
- Mainline Paving 27' width at 9" thickness
- Closest Class A aggregate source was New Ulm Quartzite (2 hour round haul)

COMPARISON: On the following page is a comparison of the crew and equipment used in a Conventional Paving operation, compared to crew and equipment that would be necessary for Composite Paving. Following that is a breakdown of the expected differences in the extra cost to place the pavement compared to the savings in producing the structural concrete.

Conventional vs. Composite Paving

Conventional

- 1 Boom Truck
- 1 Paver
- 1 Belt Placer
- 1 Cure/Texture
- 1 Skidsteer
- 1 Pickup
- 1 Service Truck
- 1 Flatbed Truck
- 1 Water Truck
- 13 Crew Members
- Assumed Mainline paving production of .90 miles per day
- Unit cost to pave/tie/green saw of $2.98 per Square Yard. $923,800 Total
- Mobilize and Operate 1 Plant
- Conventional Plant operations cost of $1.60 per Cubic Yard to batch mix.
    - Cost includes plant operator, loader, and operator

Composite

- 1 Boom Truck
- 2 Pavers
- 2 Belt Placers
- 2 Cure/Texture
- 1 Skidsteer
- 1 Pickup Truck
- 1 Service Truck
- 1 Flatbed Truck
- 1 Water Truck
- 1 Steel Bristle Broom
- 18 Crew Size
- Assumed identical production of .90 miles per day with two paver train.
- Unit cost to pave/tie/green saw of $3.70 per Square Yard. $1,147,000 Total
- Mobilize and Operate 2 Plants
    - Marginal cost to mobilize second plant $50,000 or a $.55 per cubic yard premium.
- Composite Plant operations cost of $3.82 per Cubic Yard to batch mix.
    - 2 plant operators, loader, and operator

-The Big Question is how much would the price for aggregates have to change to match the added cost of operating two paving crews and an extra batch plant?

Conventional vs. Composite Paving

Conventional Paving	

Pave, Tie, Green Saw	
Sq. Yds.	310,000
Per Sq. Yd.	$ 2.98
Total Cost	$ 923,800.00

Structural Concrete	
Cubic Yards	80,000
Per CY	$ 71.54
Total Cost	$ 5,723,200.00

TOTAL COST	$ 6,647,000.00

Composite Paving	

Pave, Tie, Green Saw	
Sq. Yds.	310,000
Per Sq. Yd.	$ 3.70
Total Cost	$ 1,147,000.00

Structural Concrete	
Cubic Yards	80,000
Per CY	$ 69.31
Total Cost	$ 5,544,800.00

TOTAL COST	$ 6,691,800.00

Total difference for the two is $44,800. The price differential is mainly due to the increased costs of placing the concrete. Laydown costs for the Composite Paving increased $.72 compared to Conventional as a result of the increased costs to run an extra paver and larger crew size. However the savings from the concrete aggregates was equal to $2.23 per cubic yard. This savings was due entirely to using recycled aggregate. These savings are achieved by crushing concrete on or near the site and using the recycled material as the main aggregate source in the thick base layer. By using substituting Recycle instead of Class A as the course aggregate material, you reduce the amount of high quality Class A aggregates needed for the job. The cost savings per ton of the recycle is between $5 and $6. Additionally, the haul time for high quality aggregates was a 2 hour round trip, but by crushing on site the haul time could be reduced to a 20 minute round. This results in just over $6 per tons savings in trucking costs. The tables below detail the difference in the amount of aggregates used as well as the cost differential between Class A and Recycled aggregates.

Conventional Aggregates	
Type	Tons
¾" Class A	34,270
1 ½" Class A	37,213
Total Tons	71,483

Composite Aggregates	
Type	Tons
¾" Class A	11,310
1 ½" Class A	12,280
Recycled Agg.	47,893
Total Tons	71,483

Class A	
Material $/Ton	$ 12.78
Trucking (2 hour)	$ 7.46
Total $ Per Ton	$ 20.24

Recycled	
Material $/Ton	$ 7.00
Trucking (20 min)	$ 1.45
Total $ Per Ton	$ 8.45

CONCLUSION: These examples were prepared using a real life project and the numbers it took to be a low bidder on the project. Our examples have shown that in the areas of the state in which Class A aggregates are not readily available or are very expensive, Composite Paving is a viable alternative to Conventional Paving. Although this example was an extreme case of having no readily available Class A aggregates, it has shown that it is possible for an alternative technique such as Composite Paving to compete to within 1% of the capabilities of a Conventional Paving process on this particular job.